18. Nanorobotics

Bradley J. Nelson, Lixin Dong

Nanorobotics is the study of robotics at the nanometer scale, and includes robots that are nanoscale in size and large robots capable of manipulating objects that have dimensions in the nanoscale range with nanometer resolution. With the ability to position and orient nanometer-scale objects, nanorobotic manipulation is a promising way to enable the assembly of nanosystems including nanorobots.

This chapter overviews the state of the art of nanorobotics, outlines nanoactuation, and focuses on nanorobotic manipulation systems and their application in nanoassembly, biotechnology and the construction and characterization of nanoelectromechanical systems (NEMS) through a hybrid approach.

Because of their exceptional properties and unique structures, carbon nanotubes (CNTs) and SiGe/Si nanocoils are used to show basic processes of nanorobotic manipulation, structuring and assembly, and for the fabrication of NEMS including nano tools, sensors and actuators.

A series of processes of nanorobotic manipulation, structuring and assembly has been demonstrated experimentally. Manipulation of individual CNTs in three-dimensional (3-D) free space has been shown by grasping using dielectrophoresis and placing with both position and orientation control for mechanical and electrical property characterization and assembly of nanostructures and devices. A variety of material property investigations can be performed, including bending, buckling, and pulling to investigate elasticity as well as strength and tribological characterization. Structuring of CNTs can be performed including shape modification, the exposure of nested cores, and connecting CNTs by van der Waals forces, electron-beam-induced deposition and mechanochemical bonding. Nanorobotics provides novel techniques for exploring the biodomain by manipulation and characterization of nanoscale objects such as cellular membranes, DNA and other biomolecules. Nano tools, sensors and actuators can provide measurements and/or movements that are calculated in nanometers, gigahertz, piconewtons, femtograms, etc., and are promising for molecular machines and bio- and nanorobotics applications. Efforts are focused on developing enabling technologies for nanotubes and other nanomaterials and structures for NEMS and nanorobotics. By combining bottom-up nanorobotic manipulation and top-down nanofabrication processes, a hybrid approach is demonstrated for creating complex 3-D nanodevices. Nanomaterial science, bionanotechnology, and nanoelectronics will benefit from advances in nanorobotics.

B. Bhushan (Ed.), *Springer Handbook of Nanotechnology*, DOI 10.1007/978-3-319-49347-3_18

18.1 Overview of Nanorobotics

Progress in robotics over the past years has dramatically extended our ability to explore the world from perception, cognition and manipulation perspectives at a variety of scales extending from the edges of the solar system down to individual atoms (Fig. 18.1). At the bottom of this scale, technology has been moving toward greater control of the structure of matter, suggesting the feasibility of achieving thorough control of the molecular structure of matter atom by atom as *Richard Feynman* first proposed in 1959 in his prophetic article on miniaturization [18.1]:

> *What I want to talk about is the problem of manipulating and controlling things on a small scale... I am not afraid to consider the final question as to whether, ultimately – in the great future – we can arrange the atoms the way we want: the very atoms, all the way down!*

He asserted that:

> *At the atomic level, we have new kinds of forces and new kinds of possibilities, new kinds of effects. The problems of manufacture and reproduction of materials will be quite different. The principles of physics, as far as I can see, do not speak against the possibility of maneuvering things atom by atom.*

This technology is now labeled *nanotechnology*.

The *great future* of Feynman began to be realized in the 1980s. Some of the capabilities he dreamed of have been demonstrated, while others are being developed. Nanorobotics represents the next stage in miniaturization for maneuvering nanoscale objects. Nanorobotics is the study of robotics at the nanometer scale, and includes robots that are nanoscale in size, i. e., nanorobots, and large robots capable of manipulating objects that have dimensions in the nanoscale range with nanometer resolution, i. e., nanorobotic manipulators. The field of nanorobotics brings together several disciplines, including nanofabrication processes used for producing nanoscale robots, nanoactuators, nanosensors, and physical modeling at nanoscales. Nanorobotic manipulation technologies, including the assembly of nanometer-sized parts, the manipulation of biological cells or molecules, and the types of robots used to perform these types of tasks also form a component of nanorobotics.

As the 21st century unfolds, the impact of nanotechnology on the health, wealth, and security of humankind is expected to be at least as significant as the combined influences in the 20th century of antibiotics, the integrated circuit, and human-made polymers. For example, *Lane* stated in 1998 [18.2]:

> *If I were asked for an area of science and engineering that will most likely produce the breakthroughs*

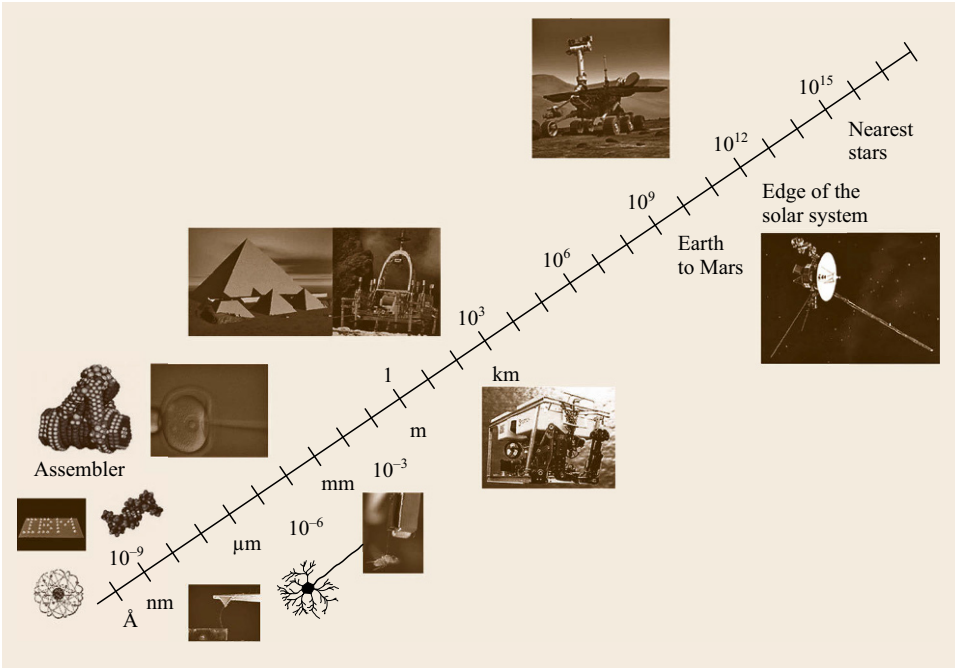

Fig. 18.1 Robotic exploration

of tomorrow, I would point to nanoscale science and engineering.

The great scientific and technological opportunities nanotechnology presents have stimulated extensive exploration of the nanoworld and initiated an exciting worldwide competition, which has been accelerated by the publication of the *National Nanotechnology Initiative* by the US government in 2000 [18.3]. Nanorobotics will play a significant role as an enabling nanotechnology and could ultimately be a core part of nanotechnology if *Drexler*'s machine-phase nanosystems based on self-replicative molecular assemblers via mechanosynthesis can be realized [18.4].

By the early 1980s, scanning tunneling microscopes (STMs) [18.5] radically changed the ways in which we interacted with and even regarded single atoms and molecules. The very nature of proximal probe methods encourages exploration of the nanoworld beyond conventional microscopic imaging. Scanned probes now allow us to perform engineering operations on single molecules, atoms, and bonds, thereby providing a tool that operates at the ultimate limits of fabrication. They have also enabled exploration of molecular properties on an individual nonstatistical basis.

STMs and other nanomanipulators are nonmolecular machines but use bottom-up strategies. Although performing only one molecular reaction at a time is obviously impractical for making large amounts of a product, it is a promising way to provide the next generation of nanomanipulators. Most importantly, it is possible to realize the directed assembly of molecules or supermolecules to build larger nanostructures through nanomanipulation. The products produced by nanomanipulation could be the first step of a bottom-up strategy in which these assembled products are used to self-assemble into nanomachines.

One of the most important applications of nanorobotic manipulation will be nanorobotic assembly. However, it appears that until assemblers capable of replication can be built, the parallelism of chemical synthesis and self-assembly are necessary when starting from atoms; groups of molecules can self-assemble quickly due to their thermal motion, enabling them to *explore* their environments and find (and bind to) complementary molecules. Given their key role in natural molecular machines, proteins are obvious candidates for early work in self-assembling artificial molecular systems. *Degrado* [18.6] demonstrated the feasibility of designing protein chains that predictably fold into solid molecular objects. Progress is also being made in artificial enzymes and other relatively small molecules that perform functions like those of natural proteins; the 1987 Nobel prize for chemistry went to *Cram* and *Lehn* for such work on supramolecular chemistry [18.7]. Several bottom-up strategies using self-assembly appear feasible [18.8]. *Fujita* et al.'s pioneering work has shown that self-assembly can be directed by adroitly exploiting the chemical and electrical bonds that hold natural molecules together, and hence get molecules to form desired nanometer-scale structures [18.9]. Chemical synthesis, self assembly, and supramolecular chemistry make it possible to provide building blocks at relatively large sizes beginning from the nanometer scale. Nanorobotic manipulation serves as the base for a hybrid approach to construct nanodevices by structuring these materials to obtain building blocks and assembling them into more complex systems.

This chapter focuses on nanorobotics including actuation, manipulation and assembly at the nanoscale. The main goal of nanorobotics is to provide an effective technology for the experimental exploration of the nanoworld, and to push the boundaries of this exploration from a robotics research perspective.

18.2 Actuation at Nanoscales

The positioning of nanorobots and nanorobotic manipulators depends largely on nanoactuators. While nanosized actuators for nanorobots are still under exploration and relatively far from implementation, microelectromechanical system (MEMS)-based efforts are focused on shrinking their sizes [18.10]. Nanometer-resolution motion has been extensively investigated and can be generated using various actuation principles. Electrostatics, electromagnetics, and piezoelectrics are the most common ways to realize actuation at nanoscales. For nanorobotic manipulation, besides nanoresolution and compact sizes, actuators generating large strokes and high forces are best suited for such applications. The speed criteria are of less importance as long as the actuation speed is in the range of a couple of hertz and above. Table 18.1 provides a small selection of early works on actuators [18.11–16] suitable in actuation principle actuators suitable for nanorobotic applications (partially adapted from [18.10]).

Several extensive reviews on various actuation principles have been published [18.17–21]. During the design of an actuator, the tradeoffs among range of motion, force, speed (actuation frequency), power

Table 18.1 Actuation with MEMS

Actuation principle	Type of motion	Volume (mm^3)	Speed (s^{-1})	Force (N)	Stroke (m)	Resolution (m)	Power density (W/m^3)	Ref.
Electrostatic	Linear	400	5000	1×10^{-7}	6×10^{-6}	n/a	200	[18.12]
Magnetic	Linear	$0.4\times0.4\times0.5$	1000	2.6×10^{-6}	1×10^{-4}	n/a	3000	[18.13]
Piezoelectric	Linear	$25.4\times12.7\times1.6$	4000	350	1×10^{-3}	7×10^{-8}	n/a	[18.14]
Actuation principle	**Type of motion**	**Volume (mm^3)**	**Speed (rad/s)**	**Torque (N m)**	**Stroke (rad)**	**Resolution (rad)**	**Power density (W/m^3)**	**Ref.**
Electrostatic	Rotational	$\pi/4\times0.5^2\times3$	40	2×10^{-7}	2π	n/a	900	[18.15]
Magnetic	Rotational	$2\times3.7\times0.5$	150	1×10^{-6}	2π	$5/36\pi$	3000	[18.16]
Piezoelectric	Rotational	$\pi/4\times1.5^2\times0.5$	30	2×10^{-11}	0.7	n/a	n/a	[18.17]

consumption, control accuracy, system reliability, robustness, load capacity, etc. must be taken into consideration. This section reviews basic actuation technologies and potential applications at nanometer scales.

18.2.1 Electrostatics

Electrostatic charge arises from a build up or deficit of free electrons in a material, which can exert an attractive force on oppositely charged objects, or a repulsive force on similarly charged objects. Since electrostatic fields arise and disappear rapidly, such devices will likewise demonstrate very fast operation speeds and be little affected by ambient temperatures.

Recent investigations have produced many examples of miniature devices using electrostatic force for actuation including silicon micro motors [18.22, 23], microvalves [18.24], and microtweezers [18.25]. This type of actuation is important for achieving nanosized actuation.

Electrostatic fields can exert great forces, but generally across very short distances. When the electric field must act over larger distances, a higher voltage will be required to maintain a given force. The extremely low-current consumption associated with electrostatic devices makes for highly efficient actuation.

18.2.2 Electromagnetics

Electromagnetism arises from electric current moving through a conducting material. Attractive or repulsive forces are generated adjacent to the conductor and proportional to the current flow. Structures can be built which gather and focus electromagnetic forces, and harness these forces to create motion.

Electromagnetic fields arise and disappear rapidly, thus permitting devices with very fast operation speeds. Since electromagnetic fields can exist over a wide range of temperatures, performance is primarily limited by the properties of the materials used in constructing the actuator.

One example of a microfabricated electromagnetic actuator is a microvalve which uses a small electromagnetic coil wrapped around a silicon micromachined valve structure [18.26]. However, the downward scalability of electromagnetic actuators into the micro- and nanorealm may be limited by the difficulty of fabricating small electromagnetic coils. Furthermore, most electromagnetic devices require perpendicularity between the current conductor and the moving element, presenting a difficulty for planar fabrication techniques commonly used to make silicon devices.

An important advantage of electromagnetic devices is their high efficiency in converting electrical energy into mechanical work. This translates into less current consumption from the power source.

18.2.3 Piezoelectrics

Piezoelectric motion arises from the dimensional changes generated in certain crystalline materials when subjected to an electric field or to an electric charge. Structures can be built which gather and focus the force of the dimensional changes, and harness them to create motion. Typical piezoelectric materials include quartz (SiO_2), lead zirconate titanate (PZT), lithium niobate, and polymers such as polyvinyledene fluoride (PVDF).

Piezoelectric materials respond very quickly to changes in voltages and with great repeatability. They can be used to generate precise motions with repeatable oscillations, as in quartz timing crystals used in many electronic devices. Piezo materials can also act as sensors, converting tension or compression strains to voltages.

On the microscale, piezoelectric materials have been used in linear inchworm drive devices [18.27], and micropumps [18.28]. STMs and most nanomanipulators use piezoelectric actuators.

Piezo materials operate with high force and speed, and return to a neutral position when unpowered. They exhibit very small strokes (under 1 %). Alternating electric currents produce oscillations in the piezo

Table 18.2 Comparison of nanoactuators

Method	Efficiency	Speed	Power density
Electrostatic	Very high	Fast	Low
Electromagnetic	High	Fast	High
Piezoelectric	Very high	Fast	High
Thermomechanical	Very high	Medium	Medium
Phase change	Very high	Medium	High
Shape memory	Low	Medium	Very high
Magnetostrictive	Medium	Fast	Very high
Electrorheological	Medium	Medium	Medium
Electrohydrodynamic	Medium	Medium	Low
Diamagnetism	High	Fast	High

material, and operation at the sample's fundamental resonant frequency produces the largest elongation and highest power efficiency [18.29]. Piezo actuators working in the stick–slip mode can provide millimeter to centimeter strokes. Most commercially available nanomanipulators adopt this type of actuators, such as Picomotors from New Focus and Nanomotors from Klock.

18.2.4 Other Techniques

Other techniques include thermomechanical, phase change, shape memory, magnetostrictive, electrorheological, electrohydrodynamic, diamagnetism, magnetohydrodynamic, shape changing, polymers, biological methods (living tissues, muscle cells, etc.) and so on. Table 18.2 lists a comparison of these.

18.3 Nanorobotic Manipulation Systems

18.3.1 Overview

Nanomanipulation, or positional and/or force control at the nanometer scale, is a key enabling technology for nanotechnology by filling the gap between top-down and bottom-up strategies, and may lead to the appearance of replication-based molecular assemblers [18.4]. These types of assemblers have been proposed as general-purpose manufacturing devices for building a wide range of useful products as well as copies of themselves (self-replication).

Presently, nanomanipulation can be applied to the scientific exploration of mesoscopic physical phenomena, biology and the construction of prototype nanodevices. It is a fundamental technology for property characterization of nanomaterials, structures and mechanisms, for the preparation of nanobuilding blocks, and for the assembly of nanodevices such as nanoelectromechanical systems (NEMS).

Nanomanipulation was enabled by the inventions of the STM [18.5], atomic force microscope (AFM) [18.30], and other types of scanning probe microscope (SPM). Besides these, optical tweezers (laser trapping) [18.31] and magnetic tweezers [18.32] are also possible nanomanipulators. Nanorobotic manipulators (NRMs) [18.33, 34] are characterized by the capability of 3-D positioning, orientation control, independently actuated multiple end-effectors, and independent real-time observation systems, and can be integrated with scanning probe microscopes. NRMs largely extend the complexity of nanomanipulation.

A concise comparison of STM, AFM, and NRM technology is shown in Fig. 18.2. With its incomparable imaging resolution, an STM can be applied to particles as small as atoms with atomic resolution. However, limited by its two-dimensional (2-D) positioning and available strategies for manipulations, standard STMs

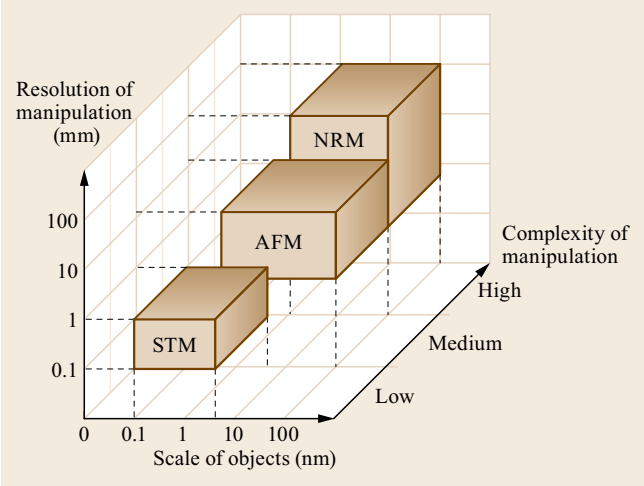

Fig. 18.2 Comparison of nanomanipulators

are ill-suited for complex manipulation and cannot be used in 3-D space. An AFM is another important type of nanomanipulator. There are three imaging modes for AFMs, i. e., contact mode, tapping mode (periodic contact mode), and non-contact mode. The latter two are also called dynamic modes and can attain higher imaging resolution than the contact mode. Atomic resolution is obtainable with non-contact mode. Manipulation with an AFM can be done in either contact or dynamic mode. Generally, manipulation with an AFM involves moving an object by touching it with a tip. A typical manipulation is like this: image a particle first in non-contact mode, then remove the tip oscillation voltage and sweep the tip across the particle in contact with the surface and with the feedback disabled. Mechanical pushing can exert larger forces on objects and, hence, can be applied for the manipulation of relatively larger objects. One-dimensional (1-D) to 3-D objects can be manipulated on a 2-D substrate. However, the manipulation of individual atoms with an AFM remains a challenge. By separating the imaging and manipulation functions, nanorobotic manipulators can have many more degrees of freedom including rotation for orientation control, and, hence, can be used for the manipulation of zero-dimensional (0-D, symmetric spheres) to 3-D objects in 3-D free space. Limited by the relative lower resolution of electron microscopes, NRMs are difficult to use for the manipulation of atoms. However, their general robotic capabilities including 3-D positioning, orientation control, independently actuated multiple end-effectors, separate real-time observation system, and integrations with SPMs inside makes NRMs quite promising for complex nanomanipulation.

The first nanomanipulation experiment was performed by *Eigler* and *Schweizer* in 1990 [18.35]. They used an STM and materials at low temperatures (4 K) to position individual xenon atoms on a single-crystal nickel surface with atomic precision. The manipulation enabled them to fabricate rudimentary structures of their own design, atom by atom. The result is the famous set of images showing how 35 atoms were moved to form the three-letter logo *IBM*, demonstrating that matter could indeed be maneuvered atom by atom as *Feynman* suggested [18.1].

A nanomanipulation system generally includes nanomanipulators as the positioning device, microscopes as *eyes*, various end-effectors including probes and tweezers among others as its *fingers*, and types of sensors (force, displacement, tactile, strain, etc.) to facilitate the manipulation and/or to determine the properties of the objects. Key technologies for nanomanipulation include observation, actuation, measurement, system design and fabrication, calibration and control, communication, and human–machine interface.

Strategies for nanomanipulation are basically determined by the environment – air, liquid or vacuum – which is further decided by the properties and size of the objects and observation methods. Figure 18.3 depicts the microscopes, environments and strategies of nanomanipulation. In order to observe manipulated objects, STMs can provide subangstrom imaging resolution, whereas AFMs can provide atomic resolution. Both can obtain 3-D surface topology. Because AFMs can be used in an ambient environment, they provide a powerful tool for biomanipulation that may require a liquid environment. The resolution of scanning electron microscopes (SEMs) is limited to about 1 nm, whereas field-emission SEMs (FESEMs) can achieve higher resolutions. SEMs/FESEMs can be used for 2-D real-time observation for both the objects and end-effectors of manipulators, and large ultrahigh-vacuum (UHV) sample chambers provide enough space to contain an NRM with many degrees of freedom (DOFs) for 3-D nanomanipulation. However, the 2-D nature of the observation makes positioning along the electron-beam direction difficult. High-resolution transmission electron microscopes (HRTEMs) can provide atomic resolution. However, the narrow UHV specimen chamber makes it difficult to incorporate large manipulators. In principle, optical microscopes (OMs) cannot be used for nanometer-scale (smaller than the wavelength of visible lights) observation because of diffraction limits. Scanning near-field OMs (SNOMs) break this limitation and are promising as a real-time observation

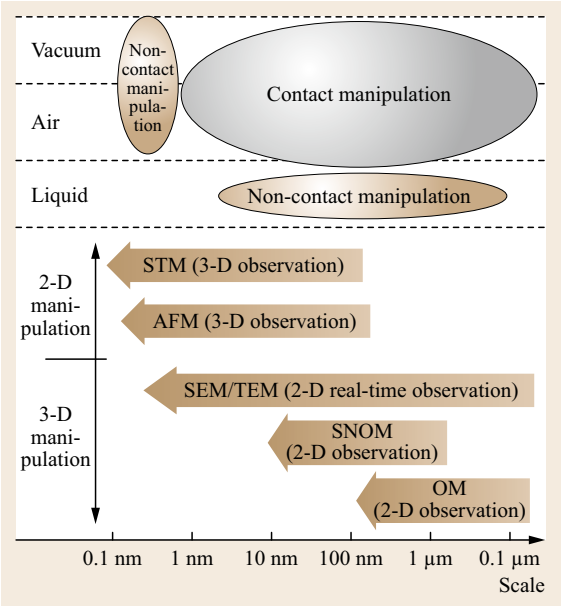

Fig. 18.3 Microscopes, environments and strategies of nanomanipulation

device for nanomanipulation, especially for ambient environments. SNOMs can be combined with AFMs, and potentially with NRMs for nanoscale biomanipulation.

Nanomanipulation processes can be broadly classified into three types: (1) lateral non-contact, (2) lateral contact, and (3) vertical manipulation. Generally, lateral non-contact nanomanipulation is mainly applied for atoms and molecules in UHV with an STM or bio-object in liquid using optical or magnetic tweezers. Contact nanomanipulation can be used in almost any environment, generally with an AFM, but is difficult for atomic manipulation. Vertical manipulation can be performed by NRMs. Figure 18.4 shows the processes of the three basic strategies.

Motion of the lateral noncontact manipulation processes are shown in Fig. 18.4a. Applicable effects [18.36] able to cause the motion include long-range van der Waals (vdW) forces (attractive) generated by the proximity of the tip to the sample [18.37], electric-field-induced fields caused by the voltage bias between the tip and the sample [18.38, 39], tunneling current local heating or inelastic tunneling vibration [18.40, 41]. With these methods, some nanodevices and molecules have been assembled [18.42, 43]. Laser trapping (optical tweezers) and magnetic tweezers are possible for non-contact manipulation of nanoorder biosamples, e.g., DNA [18.44, 45].

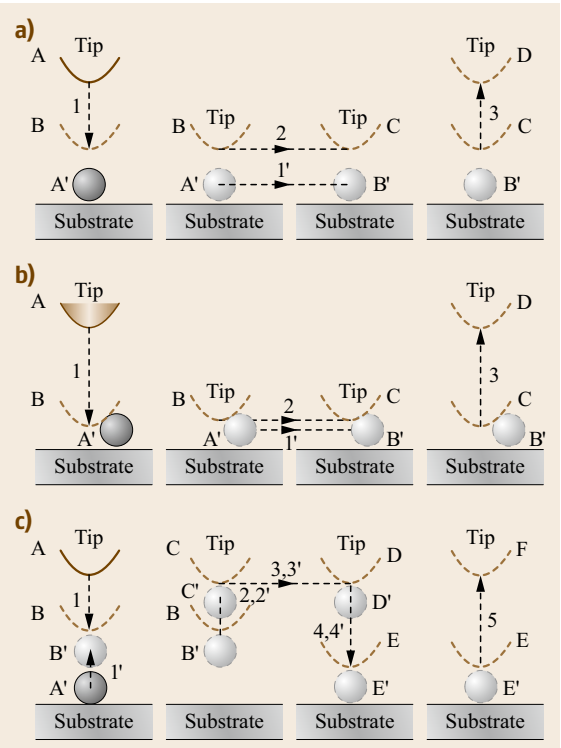

Fig. 18.4a–c Basic strategies of nanomanipulation. In the figure, A, B, C, ... represent the positions of end-effector (e.g., a tip), A′, B′, C′, ... the positions of objects, 1, 2, 3, ... the motions of end-effector, and 1′, 2′, 3′, ... the motions of objects. Tweezers can be used in pick-and-place to facilitate the picking-up, but are generally not necessarily helpful for placing. **(a)** Lateral non-contact nanomanipulation (sliding), **(b)** lateral contact nanomanipulation (pushing/pulling), **(c)** vertical nanomanipulation (picking and placing)

Non-contact manipulation combined with STMs has revealed many possible strategies for manipulating atoms and molecules. However, for the manipulation of CNTs no examples have been demonstrated.

Pushing or pulling nanometer objects on a surface with an AFM is a typical manipulation using this method as shown in Fig. 18.4b. Early work showed the effectiveness of this method for the manipulation of nanoparticles [18.46–49]. This method has also been shown in nanoconstruction [18.50] and biomanipulation [18.51]. A virtual-reality interface facilitates such manipulation [18.52, 53] and may create an opportunity for other types of manipulation. This technique has been used in the manipulation of nanotubes on a surface, and some examples will be introduced later in this chapter.

The pick-and-place task as shown in Fig. 18.4c is especially significant for 3-D nanomanipulation since its main purpose is to assemble prefabricated building blocks into devices. The main difficulty is in achieving sufficient control of the interaction between the tool and object and between the object and the substrate. Two strategies have been presented for micromanipulation [18.54] and have also proven to be effective for nanomanipulation [18.34, 55]. One strategy is to apply a dielectrophoretic force between a tool and an object as a controllable additional external force by applying a bias between the tool and the substrate on which the object is placed. Another strategy is to modify the van der Waals and other intermolecular and surface forces between the object and the substrate. For the former, an AFM cantilever is ideal as one electrode to generate a nonuniform electrical field between the cantilever and the substrate.

18.3.2 Nanorobotic Manipulation Systems

Nanorobotic manipulators are the core components of nanorobotic manipulation systems. The basic requirements for a nanorobotic manipulation system for 3-D manipulation include nanoscale positioning resolution, a relative large working space, enough DOFs including rotational ones for 3-D positioning and orientation

control of the end-effectors, and usually multiple end-effectors for complex operations.

A commercially available nanomanipulator (MM3A from Kleindiek) installed inside a SEM (Carl Zeiss DSM962) is shown in Fig. 18.5. The manipulator has three degrees of freedom, and nanometer to subnanometer-scale resolution (Table 18.3). Calculations show that, when moving/scanning in *A*/*B*-direction by joint q_1/q_2, the additional linear motion in *C* is very small. For example, when the arm length is 50 mm, the additional motion in the *C*-direction is only 0.25–1 nm when moving in the *A*-direction for 5–10 μm; these errors can be ignored or compensated with an additional motion of the prismatic joint p_3, which has a 0.25 nm resolution.

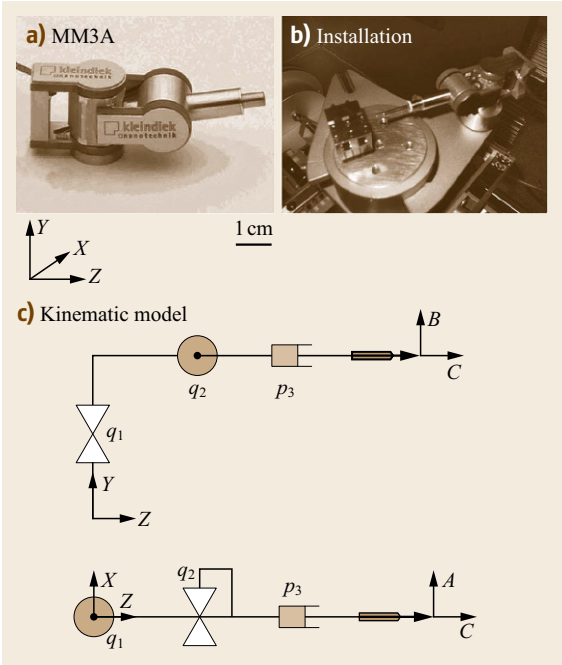

Fig. 18.5a–c Nanomanipulator (MM3A from Kleindiek) inside an SEM

Table 18.3 Specifications of MM3A

Item	Specification
Operating range q_1 and q_2	240°
Operating range *Z*	12 mm
Resolution *A* (horizontal)	10^{-7} rad (5 nm)
Resolution *B* (vertical)	10^{-7} rad (3.5 nm)
Resolution *C* (linear)	0.25 nm
Fine (scan) range *A*	20 μm
Fine (scan) range *B*	15 μm
Fine (scan) range *C*	1 μm
Speed *A*, *B*	10 mm/s
Speed *C*	2 mm/s

Figure 18.6a shows a nanorobotic manipulation system that has 16 DOFs in total and can be equipped with three to four AFM cantilevers as end-effectors for both manipulation and measurement. Table 18.4 lists the specifications of the system. Table 18.5 shows the functions of the nanorobotic manipulation system for nanomanipulation, nanoinstrumentation, nanofabrication and nanoassembly. The positioning resolution is subnanometer order and strokes are centimeter scale. The manipulation system is not only for nanomanipulation, but also for nanoassembly, nanoinstrumentation and nanofabrication. Four-probe semiconductor measurements are perhaps the most complex manipulation this system can perform, because it is necessary to actuate four probes independently by four manipulators. Theoretically, 24 DOFs are needed for four manipulators for general-purpose manipulations, i. e., 6 DOFs for each manipulator for complete control of three linear DOFs and three rotation DOFs. However, 16 DOFs are sufficient for this specific purpose. In general, two manipulators are sufficient for most tasks. More probes

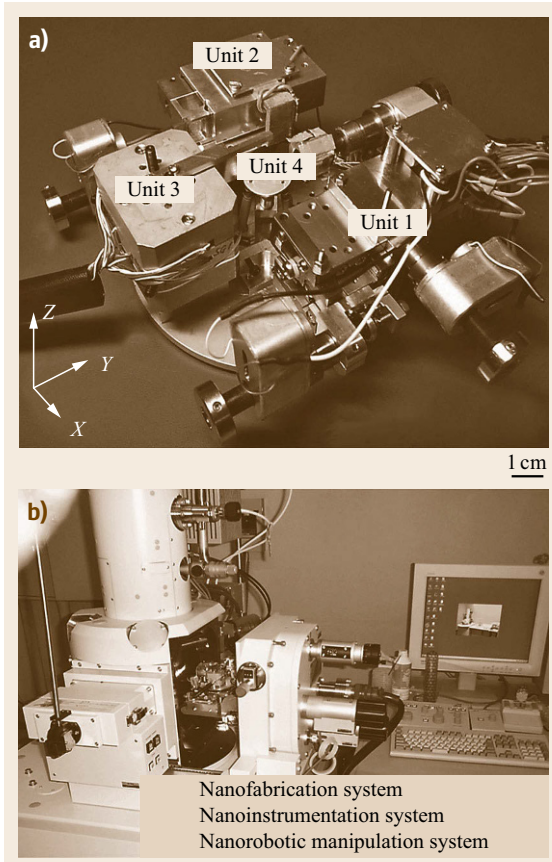

Fig. 18.6a,b Nanorobotic system. **(a)** Nanorobotic manipulators, **(b)** system setup

Table 18.4 Specifications of a nanorobotic manipulation system

Item	Specification
Nanorobotic manipulation system	
DOFs	Total: 16 DOFs
	Unit 1: 3 DOFs (x, y and β; coarse)
	Unit 2: 1 DOF (z; coarse), 3-DOF (x, y and z; fine)
	Unit 3: 6 DOFs (x, y, z, α, β, γ; ultrafine)
	Unit 4: 3 DOFs (z, α, β; fine)
Actuators	4 Picomotors (Units 1 & 2)
	9 PZTs (Units 2 & 3)
	7 Nanomotors (Units 2 & 4)
End-effectors	3 AFM cantilevers + 1 substrate or
	4 AFM cantilevers
Working space	18 mm × 18 mm × 12 mm × 360° (coarse, fine),
	26 μm × 22 μm × 35 μm (ultrafine)
Positioning resolution	30 nm (coarse), 2 mrad (coarse), 2 nm (fine), sub-nm (ultrafine)
Sensing system	FESEM (imaging resolution: nm) and AFM cantilevers
Nanoinstrumentation system	
FESEM	Imaging resolution: 1.5 nm
AFM cantilever	Stiffness constant: 0.03 nN/nm
Nanofabrication system	
EBID	FESEM emitter: T-FE
	CNT emitter

Table 18.5 Functions of a nanorobotic manipulation system

Functions	Manipulations involved
Nanomanipulation	Picking up nanotubes by controlling intermolecular and surface forces, and positioning them together in 3-D space
Nanoinstrumentation	Mechanical properties: buckling or stretching
	Electrical properties: placing between two probes (electrodes)
Nanofabrication	EBID with a CNT emitter and parallel EBID
	Destructive fabrication: breaking
	Shape modification: deforming by bending and buckling, and fixing with EBID
Nanoassembly	Connecting with van der Waals
	Soldering with EBID
	Bonding through mechanochemical synthesis

provide for more potential applications. For example, three manipulators can be used to assemble a nanotube transistor, a third probe can be applied to cut a tube supported on the other two probes, four probes can be used for four-terminal measurements to characterize the electric properties of a nanotube or a nanotube cross-junction. There are many potential applications for the manipulators if all four probes are used together. With the advancement of nanotechnology, one could shrink the size of nanomanipulators and insert more DOFs inside the limited vacuum chamber of a microscope, and, perhaps, the molecular version of manipulators such as that dreamed of by *Drexler* could be realized [18.4].

For the construction of multiwalled carbon nanotubes (MWNT)-based nanostructures, manipulators position and orient nanotubes for the fabrication of nanotube probes and emitters, for performing na-

nosoldering with electron-beam-induced deposition (EBID) [18.56], for the property characterization of single nanotubes for selection purposes and for characterizing junctions to test connection strength.

A nanolaboratory is shown in Fig. 18.6b, and its specifications are listed in Table 18.4. The nanolaboratory integrates a nanorobotic manipulation system with a nano analytical system and a nanofabrication system, and can be applied for manipulating nanomaterials, fabricating nanobuilding blocks, assembling nanodevices, and for in situ analysis of the properties of such materials, building blocks and devices. Nanorobotic manipulation within the nanolaboratory has opened a new path for constructing nanosystems in 3-D space, and will create opportunities for new nanoinstrumentation and nanofabrication processes.

18.4 Nanorobotic Assembly

18.4.1 Overview

Nanomanipulation is a promising strategy for nanoassembly. Key techniques for nanoassembly include the structuring and characterization of nanobuilding blocks, the positioning and orientation control of the building blocks with nanometer-scale resolution, and effective connection techniques. Nanorobotic manipulation, which is characterized by multiple DOFs with both position and orientation controls, independently actuated multi-probes, and a real-time observation system, have been shown to be effective for assembling nanotube-based devices in 3-D space.

The well-defined geometries, exceptional mechanical properties, and extraordinary electric characteristics, among other outstanding physical properties (as listed in Table 18.6), of CNTs [18.57] qualify them for many potential applications (as concisely listed in Table 18.7), especially in nanoelectronics [18.58–60], NEMS, and other nanodevices [18.61]. For NEMS, some of the most important characteristics of nanotubes include their nanometer diameter [18.62], large aspect ratio (10−1000) [18.63, 64], TPa-scale Young's modulus [18.65–71], excellent elasticity [18.33, 72], ultrasmall interlayer friction, excellent capability for field emission, various electric conductivities [18.73–75], high thermal conductivity [18.76], high current-carrying capability with essentially no heating [18.77, 78], sensitivity of conductance to various physical or chemical changes, and charge-induced bond-length change.

Helical 3-D nanostructures, or nanocoils, have been synthesized from various materials, including helical carbon nanotubes [18.79] and zinc oxide nanobelts [18.80]. A new method of creating structures with nanometer-scale dimensions has recently been presented [18.81] and can be fabricated in a controllable way [18.82]. The structures are created through a top-down fabrication process in which a strained nanometer-thick heteroepitaxial bilayer curls up to form 3-D structures with nanoscale features. Helical geometries and tubes with diameters between 10 nm and 10 μm have been achieved. Because of their interesting morphology, mechanical, electrical, and electromagnetic properties, potential applications of these nanostructures in NEMS include nanosprings [18.83], electromechanical sensors [18.84], magnetic-field detectors, chemical or biological sensors, generators of magnetic beams, inductors, actuators, and high-performance electromagnetic-wave absorbers.

Table 18.6 Properties of carbon nanotubes

Property	Item	Data
Geometrical	Layers	Single/multiple
	Aspect ratio	10−1000
	Diameter	≈ 0.4 nm to > 3 nm (SWNTs)
		≈ 1.1 to > 100 nm (MWNTs)
	Length	Several μm (rope up to cm)
Mechanical	Young's modulus	≈ 1 TPa (steel: 0.2 TPa)
	Tensile strength	45 GPa (steel: 2 GPa)
	Density	1.33−1.4 g/cm^3 (Al: 2.7 g/cm^3)
Electronic	Conductivity	Metallic/semiconductivity
	Current carrying Capacity	≈ 1 TA/cm^3 (Cu: 1 GA/cm^3)
	Field emission	Activate phosphorus at 1−3 V
Thermal	Heat transmission	> 3 kW/(m K) (diamond: 2 kW/(m K))

Table 18.7 Applications of carbon nanotubes

State	Device	Main properties applied
Bulk/array	Composite	High strength, conductivity, etc.
	Field emission devices: flat display, lamp, gas discharge tube, x-ray source, microwave generator, etc.	Field emission: stable emission, long lifetimes, and low emission threshold potentials, high current densities
	Electrochemical devices: supercapacitor, battery cathode, electromechanical actuator, etc.	Large surface area conductivity, high strength, high reversible component of storage capacity
	Fuel cell, hydrogen storage, etc.	Large surface area
Individual	Nanoelectronics: wire, diode, transistor, switch memory, etc.	Small sizes, semiconducting/metallic
	NEMS: probe, tweezers, scissors, sensor, actuator, bearing, gear, etc.	Well-defined geometrics, exceptional mechanical and electronic properties

NEMS based on individual single- or multi-walled carbon nanotubes (SWNTs [18.85, 86] or MWNTs [18.57]) and nanocoils are of increasing interest, indicating that capabilities for incorporating these individual building blocks at specific locations on a device must be developed. Random spreading [18.87], direct growth [18.88], self-assembly [18.89], dielectrophoretic assembly [18.90] and nanomanipulation [18.91] have been demonstrated for positioning as-grown nanotubes on electrodes for the construction of these devices. However, for nanotube-based structures, nanorobotic assembly is still the only technique capable of in situ structuring, characterization and assembly. Because the as-fabricated nanocoils are not free-standing from their substrate, nanorobotic assembly is virtually the only way to incorporate them into devices at present.

18.4.2 Carbon Nanotubes

Nanotube manipulation in two dimensions on a surface was first performed with an AFM by contact pushing on a substrate. Figure 18.7 shows the typical methods for 2-D pushing. Although similar to that shown in Fig. 18.4b, the same manipulation caused various results because nanotubes cannot be regarded as 0-D points. The first demonstration was given by *Lieber* and coworkers for measuring the mechanical properties of a nanotube [18.66]. They used the method shown in Fig. 18.7b, i. e., bending a nanotube by pushing on one end of it and fixing the other end. The same strategy was used for the investigation of the behaviors of nanotubes under large strain [18.92]. *Dekker* and coworkers applied the strategies shown in Fig. 18.7c,d to get a kinked junction and crossed nanotubes [18.93, 94]. *Avouris* and coworkers combined this technique with an inverse process, namely straightening by pushing along a bent tube, and realized the translation of the tube to another location [18.95] and between two electrodes to measure the conductivity [18.96], and to form a field-effect transistor (FET) [18.97]. This technique was also used to place a tube on another tube to form a single electron transistor (SET) with cross-junction of nanotubes [18.98]. Pushing-induced breaking (Fig. 18.7d) has also been demonstrated for an adsorbed nanotube [18.95] and a freely suspended SWNT rope [18.72]. The simple assembly of two bent tubes and a straight one formed the Greek letter θ.

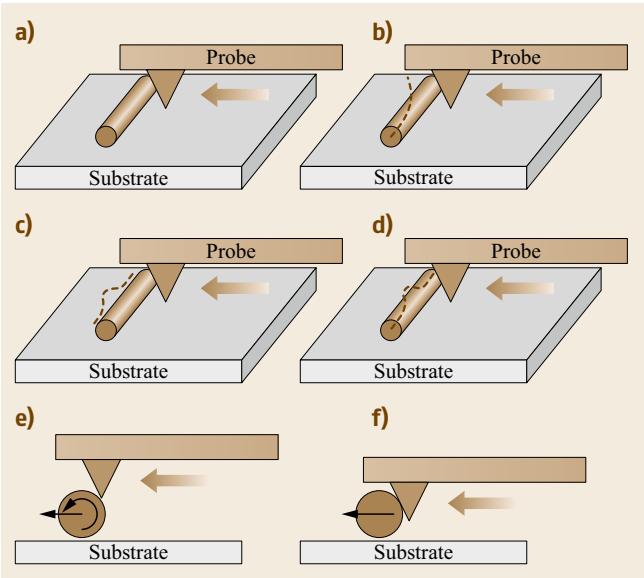

Fig. 18.7a–f 2-D manipulation of CNTs. Starting from the original state shown in **(a)**, pushing the tube at a different site with a different force may cause the tube to deform as in **(b)** and **(c)**, to break as in **(d)**, or to move as in **(e)** and **(f)**. **(a)** Original state, **(b)** bending, **(c)** kinking, **(d)** breaking, **(e)** rolling, **(f)** sliding

To investigate the dynamics of rolling at the atomic level, rolling and sliding of a nanotube (as shown in Fig. 18.7e,f) are performed on graphite surfaces using an AFM [18.99, 100].

Manipulation of CNTs in 3-D space is important for assembling CNTs into structures and devices. The basic techniques for the nanorobotic manipulation of carbon nanotubes are shown in Fig. 18.8 [18.101]. These serve as the basis for handling, structuring, characterizing and assembling NEMS.

The basic procedure is to pick up a single tube from nanotube soot, Fig. 18.8a. This has been shown first by using dielectrophoresis [18.34] through nanorobotic manipulation (Fig. 18.8b). By applying a bias between a sharp tip and a plane substrate, a nonuniform electric field can be generated between the tip and the substrate with the strongest field near the tip. This field can cause a tube to orient along the field or further *jump* to the tip by electrophoresis or dielectrophoresis (determined by the conductivity of the objective tubes). Removing the bias, the tube can be placed at other locations at will. This method can be used for free-standing tubes on nanotube soot or on a rough surface on which surface van der Waals forces are generally weak. A tube strongly rooted in CNT soot or lying on a flat surface cannot be picked up in this way. The interaction be-

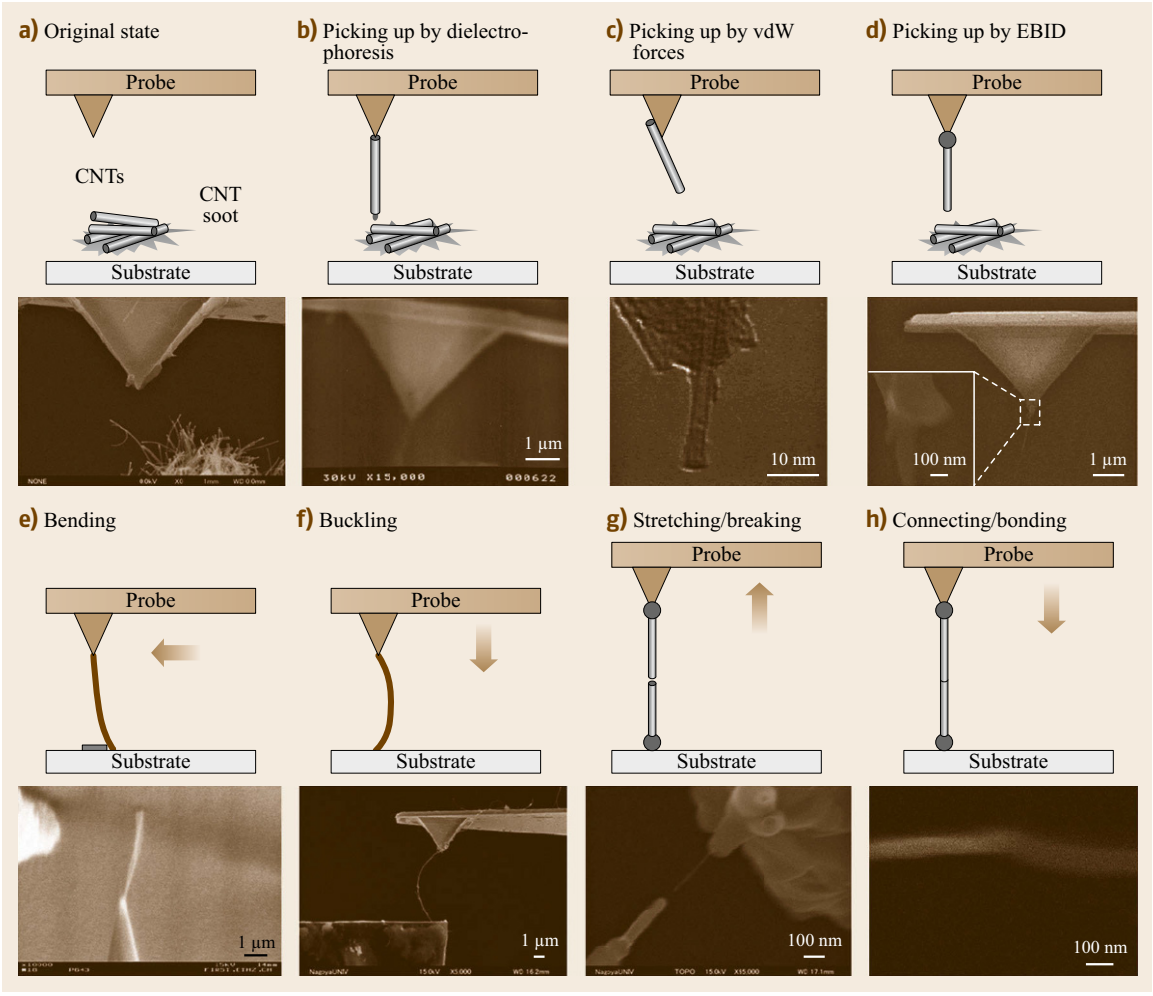

Fig. 18.8a–h Nanorobotic manipulation of CNTs. The basic technique is to pick up an individual tube from CNT soot **(a)** or from an oriented array; **(b)** shows a free-standing nanotube picked up by dielectrophoresis generated by a nonuniform electric field between the probe and substrate, **(c)** (after [18.102]) and **(d)** show the same manipulation by contacting a tube with the probe surface or fixing (e.g., with EBID) a tube to the tip (*inset* shows the EBID deposit). Vertical manipulation of nanotubes includes bending **(e)**, buckling **(f)**, stretching/breaking **(g)**, and connecting/bonding **(h)**. All examples with the exception of **(c)** are from the authors' work

tween a tube and the atomically flat surface of the AFM cantilever tip has been shown to be strong enough to pick up a tube with the tip [18.102] (Fig. 18.8c). By using EBID, it is possible to pick up and fix a nanotube onto a probe [18.103] (Fig. 18.8d). For handling a tube, a weak connection between the tube and the probe is desired.

Bending and buckling a CNT as shown in Fig. 18.8e,f are important for in situ property characterization of a nanotube [18.104, 105], which is a simple way to get the Young's modulus of a nanotube without damaging the tube (if performed within its elastic range) and, hence, can be used for the selection of a tube with desired properties. The process is shown in Fig. 18.9a. The left figure shows an individual MWNT, whereas the right four show a bundle of MWNTs being buckled. Figure 18.9b depicts the property curve of the elastic and plastic deformations of the MWNT ($\varnothing 133\,\text{nm} \times 6.055\,\mu\text{m}$), where d and F are the axial deformation and buckling force, as shown in Fig. 18.9a (top). By using the model and analysis method presented in [18.55], the flexural rigidity of the MWNT bundle shown in Fig. 18.9a (bottom) is found to be $EI = 2.086 \times 10^{-19}\,[\text{N m}^2]$. This result suggests that the diameter of the nanotube is 46.4 nm if the theoretical value of the Young's modulus of the nanotube $E = 1.26\,\text{TPa}$ is used. The SEM image shows that the bundle of nanotubes includes at least three single ones with diameters of 31, 34, and 41 nm. Hence, it can be determined that there must be damaged parts in the bundle because the stiffness is too low, and it is necessary to select another one without defects. By buckling an MWNT over its elastic limit, a kinked structure can be obtained. After three loading/releasing rounds, as shown in Fig. 18.9b, a kinked structure is obtained, as shown in Fig. 18.10a [18.106]. To obtain any desired angle for a kinked junction it is possible to fix the shape of a buckled nanotube within its elastic limit by using EBID (Fig. 18.10b) [18.107]. For a CNT, the maximum angular displacement will appear at the fixed left end under pure bending or at the middle point under pure buckling. A combination of these two kinds of loads will achieve a controllable position of the kink point and a desired kink angle θ. If the deformation is within the elastic limit of the nanotube, it will recover as the load is released. To avoid this, EBID can be applied at the kink point to fix the shape.

Stretching a nanotube between two probes or a probe and a substrate has generated several interesting results (Fig. 18.8g). The first demonstration of 3-D nanomanipulation of nanotubes took this as an example to show the breaking mechanism of an MWNT [18.33], and to measure the tensile strength of CNTs [18.71]. By breaking an MWNT in a controlled manner, interesting nanodevices have been fabricated. This technique – destructive fabrication – has been presented to get sharpened and layered structures of nanotubes and to improve control of the length of nanotubes [18.108]. Typically, a layered and a sharpened structure can be obtained from this process, similar to that achieved from electric pulses [18.109]. Bearing motion has also been observed in an incompletely broken MWNT (Fig. 18.11). As shown in Fig. 18.11a, an MWNT is supported between a substrate (left end) and an AFM cantilever (right end). Figure 18.11b shows a zoomed image of the centrally blocked part of Fig. 18.11a, and the inset shows its structure schematically. It can be found that the nanotube has a thinner neck (part B in Fig. 18.11b) that was formed by destructive fabrication, i. e., by moving the cantilever to the right. To move it further in the same direction, a motion like a linear bearing is observed, as shown in Fig. 18.11c and schematically by the inset. By comparing Fig. 18.11b,c, we find that part B remained

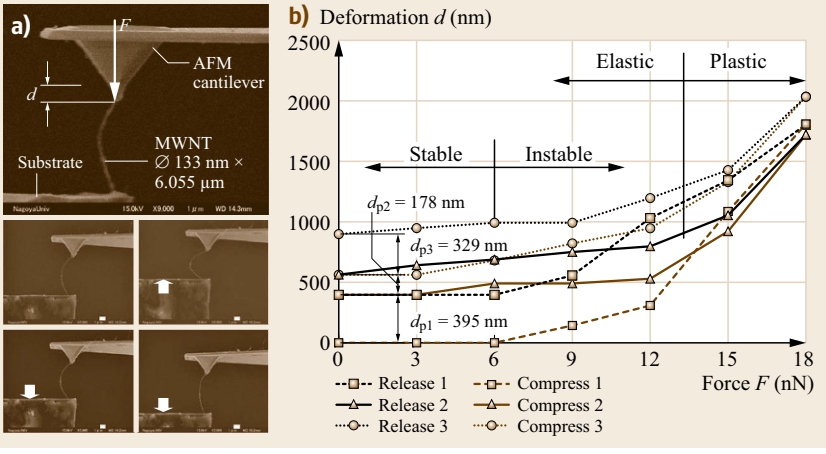

Fig. 18.9a,b In-situ mechanical property characterization of a nanotube by buckling it (scale bars: 1 μm). **(a)** Process of buckling, **(b)** elastic and plastic properties of an MWNT

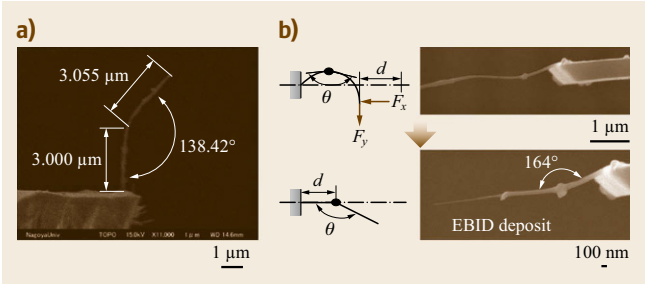

Fig. 18.10a,b Shape modification. **(a)** Kinked structure of a MWNT through plastic deformation, **(b)** shape modifications of a MWNT by elastic bending and buckling deformation and shape fixing through EBID

unchanged in its length and diameter, while its two ends brought out two new parts I and II from parts A and B, respectively. Part II has uniform diameter (∅ 22 nm), while part I is a tapered structure with a smallest diameter of ∅ 25 nm. The interlayer friction has been predicted to be very small [18.110], but direct measurement of the friction remains a challenging problem.

The reverse process, namely the connection of broken tubes (Fig. 18.8h), has been demonstrated recently, and the mechanism is revealed as rebonding of unclosed dangling bonds at the ends of broken tubes [18.111]. Based on this interesting phenomenon, mechanochemical nanorobotic assembly has been performed [18.112].

Assembly of nanotubes is a fundamental technology for enabling nanodevices. The most important tasks include the connection of nanotubes and placing of nanotubes onto electrodes. Pure nanotube circuits [18.113–115] created by interconnecting nanotubes of different diameters and chirality could lead to further size reductions in devices. Nanotube intermolecular and intramolecular junctions are basic elements for such systems. An intramolecular kink junction behaving like a rectifying diode has been reported [18.116]. Room-temperature (RT) SETs [18.117] have been shown with a short (≈ 20 nm) nanotube section that is created by inducing local barriers into the tube with an AFM, and Coulomb charging has been observed. With a cross-junction of two SWNTs (semiconducting/metallic), three- and four-terminal electronic devices have been

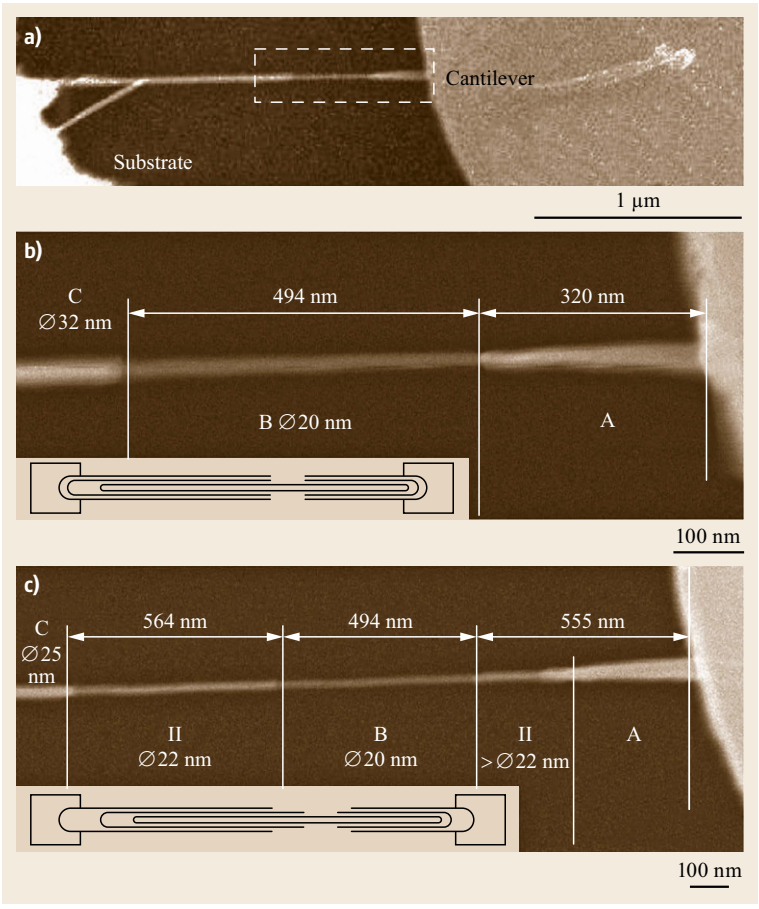

Fig. 18.11a–c Destructive fabrication of a MWNT and its bearing-like motion

made [18.118]. A suspended cross-junction can function as electromechanical nonvolatile memory [18.119].

Although some kinds of junctions have been synthesized with chemical methods, there is no evidence yet showing that a self-assembly-based approach can provide more complex structures. SPMs were also used to fabricate junctions, but they are limited to a 2-D plane. We have presented 3-D nanorobotic manipulation-based nanoassembly, which is a promising strategy, both for the fabrication of nanotube junctions and for the construction of more complex nanodevices with such junctions as well.

Nanotube junctions can be classified into different types by: the kind of components – SWNTs or MWNTs; geometric configuration – V (kink), I, X- (cross), T-, Y- (branch), and 3-D junctions; conductivity – metallic or semiconducting; and connection methods – intermolecular (connected with van der Waals force, EBID, etc.) or intramolecular (connected with chemical bonds) junctions. Here we show the fabrication of several kinds of MWNT junctions by emphasizing the connection methods. These methods will also be effective for SWNT junctions. Figure 18.12 shows CNT junctions constructed by connecting with van der Waals forces (a), joining by electron-beam-induced deposition (b), and bonding through mechanochemistry (c).

MWNT junctions connected with van der Waals forces are the basic forms of junctions. To fabricate such junctions, the main process is to position two or more nanotubes together with nanometer resolution; they will then be connected naturally by intermolecular van der Waals forces. Such junctions are mainly for structures where contact rather than strength is emphasized. Placing them onto a surface can make them more stable. In some cases, when lateral movement along the surface of nanotubes is desired while keeping them in contact, van der Waals-type connections are the only ones that are suitable.

Figure 18.12a shows a T-junction connected with van der Waals forces, which is fabricated by positioning the tip of an MWNT onto another MWNT until they form a bond. The contact is checked by measuring the shear connection force.

EBID provides a soldering method to obtain stronger nanotube junctions than those connected through van der Waals forces. Hence, if the strength of nanostructures is emphasized, EBID can be applied. Figure 18.12b shows an MWNT junction connected through EBID, in which the upper MWNT is a single one with a diameter of 20 nm and the lower one is a bundle of MWNTs with an extruded single CNT with ∅30 nm. The development of conventional EBID has been limited by the expensive electron filament used and low productivity. We have presented a parallel EBID system by using CNTs as emitters because of their excellent field-emission properties [18.120, 121]. The feasibility of parallel EBID is presented. It is a promising strategy for large-scale fabrications of nanotube junctions. Similar to its macro counterpart, welding, EBID works by adding material to obtain stronger connections, but in some cases, added material might influence normal functions for nanosystems. So, EBID is mainly applied to nanostructures rather than nanomechanisms.

To construct stronger junctions without adding additional material, mechanochemical nanorobotic assembly is an important strategy. Mechanochemical nanorobotic assembly is based on solid-phase chemical reactions, or mechanosynthesis, which is defined as chemical synthesis controlled by mechanical systems operating with atomic-scale precision, enabling direct positional selection of reaction sites [18.4]. By picking up atoms with dangling bonds rather than natural atoms only, it is easier to form primary bonds, which provides a simple but strong connection. Destructive fabrication provides a way to form dangling bonds at the ends of broken tubes. Some of the dangling bonds may close with neighboring atoms, but generally a few bonds will remain dangling. A nanotube with dangling bonds at its end will bind more easily to another

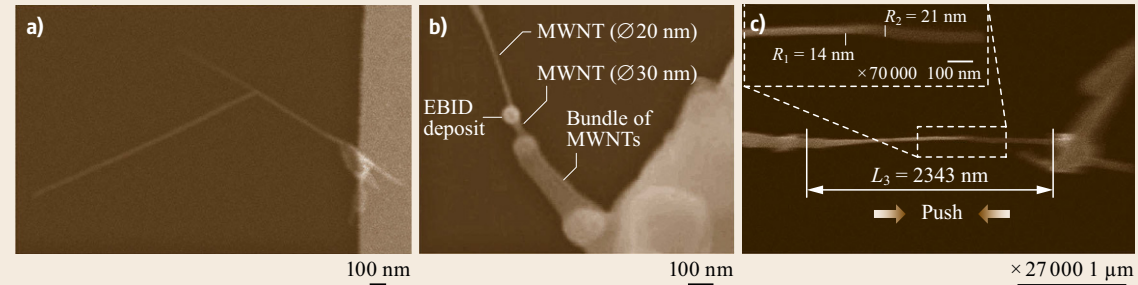

Fig. 18.12a–c MWNT junctions. **(a)** MWNTs connected with van der Waals force. **(b)** MWNTs joined with EBID. **(c)** MWNTs bonded with a mechanochemical reaction

to form intramolecular junctions. Figure 18.12c shows such a junction. An MWNT (length $L_1 = 1329\,\text{nm}$, diameter $D_1 = 42\,\text{nm}$) is placed between a substrate and an AFM cantilever with a CNT tip, and the two ends are fixed. By pulling the two ends of the MWNT, it is broken into two parts. By pushing the two nanotubes head to head close enough, a new one is formed. To test the strength of this nanotube, it was broken again. The fact that the nanotube breaks at a different site suggests that the tensile strength of the connected nanotubes is not weaker than that of the original nanotube itself. We have determined that no type of connection based on van der Waals interactions can provide such a strong connection strength [18.112]. Also, we have shown that, from the measured tensile strength (1.3 TPa), chemical bonds must have been formed when the junction formed, and that these are most likely to be covalent bonds (sp^2-hybrid type, as in a nanotube).

3-D nanorobotic manipulation has opened a new route for structuring and assembly nanotubes into nanodevices. However, at present nanomanipulation is still performed in a serial manner with master–slave control, which is not a large-scale production-oriented technique. Nevertheless, with advances in the exploration of mesoscopic physics, better control of the synthesis of nanotubes, more accurate actuators, and effective tools for manipulation, high-speed and automatic nanoassembly will be possible. Another approach might be parallel assembly by positioning building blocks with an array of probes [18.122] and joining them together simultaneously, e.g., with the parallel EBID [18.103] approach we presented. Further steps might progress towards exponential assembly [18.123], and in the far future to self-replicating assembly [18.4].

18.4.3 Nanocoils

The construction of nanocoil-based NEMS involves the assembly of as-grown or as-fabricated nanocoils, which is a significant challenge from a fabrication standpoint. Focusing on the unique aspects of manipulating nanocoils due to their helical geometry, high elasticity, single end fixation, and strong adhesion to the substrate from wet etching, a series of new processes is presented using a manipulator (MM3A, Kleindiek) installed in an SEM (Zeiss DSM962). As-fabricated SiGe/Si bilayer nanocoils are shown in Fig. 18.13. Special tools have been fabricated including a nanohook prepared by controlled *tip-crashing* of a commercially available tungsten sharp probe (Picoprobe T-4-10-1 mm and T-4-10) onto a substrate, and a *sticky* probe prepared by tip dipping into a double-sided SEM silver conductive tape (Ted Pella, Inc.). As shown in Fig. 18.14, experiments demonstrate that nanocoils can be released from a chip by

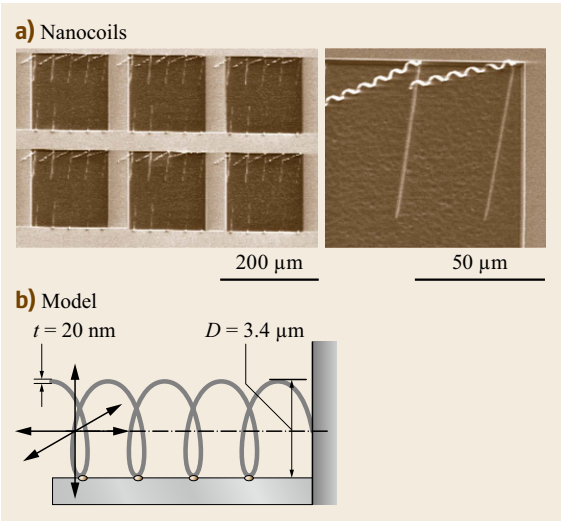

Fig. 18.13a,b As-fabricated nanocoils with a thickness of $t = 20\,\text{nm}$ (without Cr layer) or 41 nm (with Cr layer). Diameter: $D = 3.4\,\mu\text{m}$

lateral pushing, picked up with a nanohook or a *sticky* probe, and placed between the probe/hook and another probe or an AFM cantilever (Nanoprobe, NP-S). Axial pulling/pushing, radial compressing/releasing, and bending/buckling have also been demonstrated. These processes have shown the effectiveness of manipulation for the characterization of coil-shaped nanostructures and their assembly for NEMS, which have been otherwise unavailable.

Configurations of nanodevices based on individual nanocoils are shown in Fig. 18.15. Cantilevered nanocoils as shown in Fig. 18.15a can serve as nanosprings. Nanoelectromagnets, chemical sensors and nanoinductors involve nanocoils bridged between two electrodes, as shown in Fig. 18.15b. Electromechanical sensors can use a similar configuration but with one end connected to a moveable electrode, as shown in Fig. 18.15c. Mechanical stiffness and electric conductivity are fundamental properties for these devices that must be further investigated.

As shown in Fig. 18.14h, axial pulling is used to measure the stiffness of a nanocoil. A series of SEM images are analyzed to extract the AFM tip displacement and the nanospring deformation, i. e., the relative displacement of the probe from the AFM tip. From this displacement data and the known stiffness of the AFM cantilever, the tensile force acting on the nanospring versus the nanospring deformation was plotted. The deformation of the nanospring was measured relative to the first measurement point. This was necessary because proper attachment of the nanospring to the AFM cantilever must be verified. Afterwards, it was not pos-

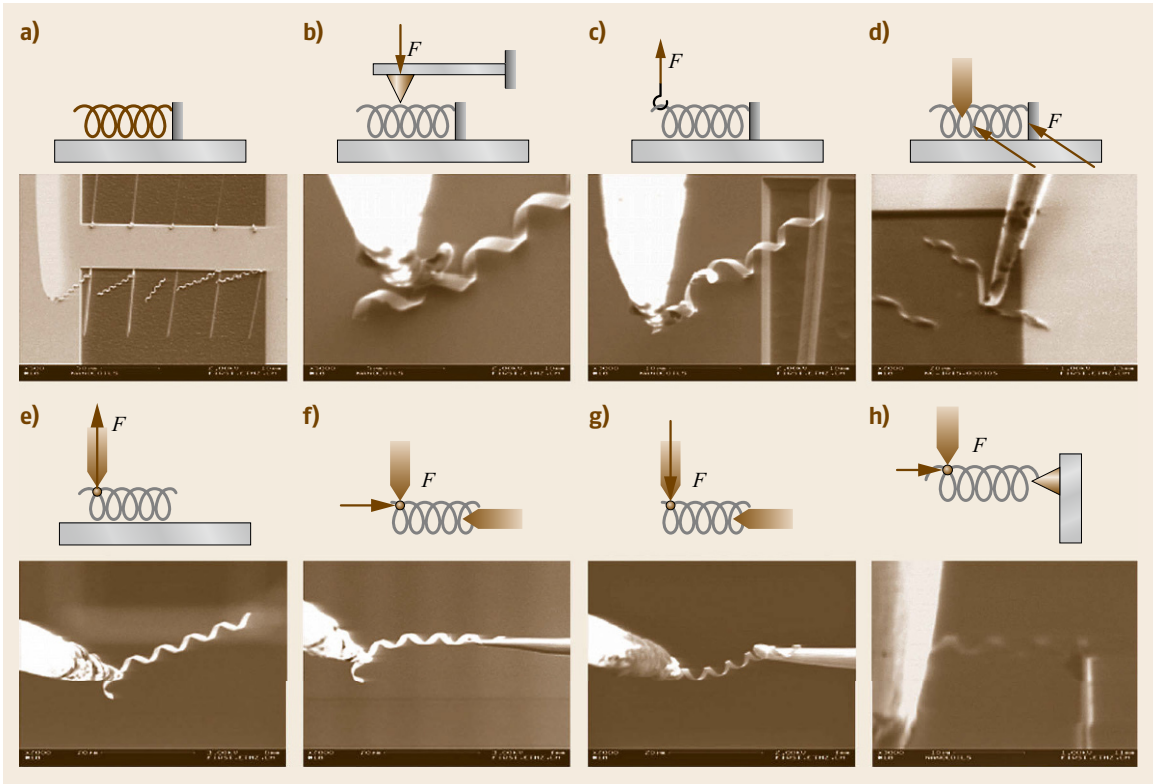

Fig. 18.14a–h Nanorobotic manipulation of nanocoils: **(a)** original state, **(b)** compressing/releasing, **(c)** hooking, **(d)** lateral pushing/breaking, **(e)** picking, **(f)** placing/inserting, **(g)** bending, and **(h)** pushing and pulling

sible to return to the point of zero deformation. Instead, the experimental data, as presented in Fig. 18.15d, has been shifted such that, with the calculated linear elastic spring stiffness, the line begins at zero force and zero deformation. From Fig. 18.15d, the stiffness of the spring was estimated to be 0.0233 N/m. The linear elastic region of the nanospring extends to a deformation of 4.5 μm. An exponential approximation was fitted to the nonlinear region. When the applied force reached 0.176 μN, the attachment between the nanospring and the AFM cantilever broke. Finite element simulation (ANSYS 9.0) was used to validate the experimental data [18.84]. Since the exact region of attachment cannot be identified according to the SEM images, simulations were conducted for 4, 4.5, and 5 turns to get an estimate of the possible range, given that the apparent number of turns of the nanospring is between 4 and 5. The nanosprings in the simulations were fixed on one end and had an axial load of 0.106 μN applied to the other end. The simulation results for the spring with 4 turns yield a stiffness of 0.0302 N/m; for the nanospring with 5 turns it is 0.0191 N/m. The measured stiffness falls into this range at 22.0% above the minimum value and 22.8% below the maximum value, and very close to the stiffness of a 4.5 turn nanospring, which has a stiffness of 0.0230 N/m according to the simulation.

Figure 18.15e shows the results from electrical characterization experiments on a nanospring with 11 turns using the configuration as shown in Fig. 18.14g. The *I*–*V* curve is nonlinear, which may be caused by the resistance change of the semiconductive bilayer due to ohmic heating. Another possible reason is the decrease in contact resistance caused by thermal stress. The maximum current was found to be 0.159 mA under an 8.8 V bias. Higher voltage causes the nanospring to *blow off*. From the fast scanning screen of the SEM, the extension of the nanospring on the probes was observed around the peak current so that the current does not drop abruptly. At 9.4 V, the extended nanospring is broken down, causing an abrupt drop in the *I*–*V* curve.

From fabrication and characterization results, the helical nanostructures appear to be suitable to function as inductors. They would allow further miniaturization compared to state-of-the-art microinductors. For this purpose, higher doping of the bilayer and an additional metal layer would result in the required conductance. Conductance, inductance, and quality factor can be

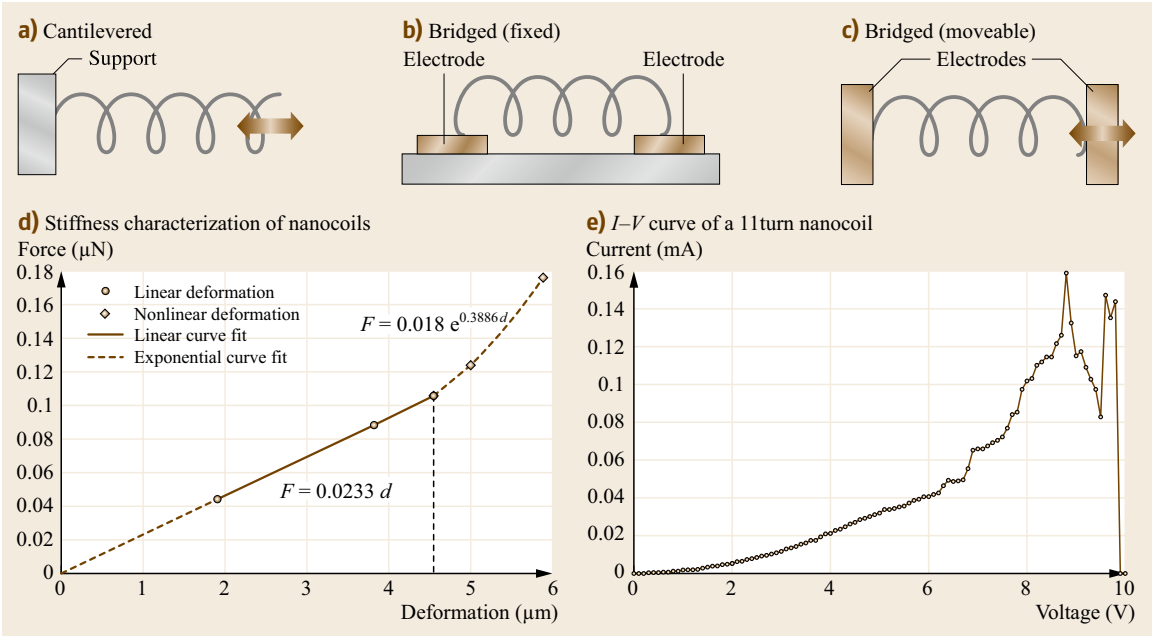

Fig. 18.15a–e Nanocoil-based devices. Cantilevered nanocoils **(a)** can serve as nanosprings. Nanoelectromagnets, chemical sensors, and nanoinductors involve nanocoils bridged between two electrodes **(b)**. Electromechanical sensors can use a similar configuration but with one end connected to a moveable electrode **(c)**. Mechanical stiffness **(d)** and electric conductivity **(e)** are basic properties of interest for these devices

further improved if, after curling up, additional metal is electroplated onto the helical structures. Moreover, a semiconductive helical structure, when functionalized with binding molecules, can be used for chemical sensing using the same principle as demonstrated with other types of nanostructures [18.124]. With bilayers in the range of a few monolayers, the resulting structures would exhibit a very high surface-to-volume ratio with the whole surface exposed to an incoming analyst.

18.5 Applications

Material science, biotechnology, electronics, and mechanical sensing and actuation will benefit from advances in nanorobotics. Research topics in bionanorobotics include the autonomous manipulation of single cells or molecules, the characterization of biomembrane mechanical properties using nanorobotic systems with integrated vision and force-sensing modules, and more. The objective is to obtain a fundamental understanding of single-cell biological systems and provide characterized mechanical models of biomembranes for deformable cell tracking during biomanipulation and cell injury studies. Robotic manipulation at nanometer scales is a promising technology for structuring, characterizing and assembling nanobuilding blocks into NEMS. Combined with recently developed nanofabrication processes, a hybrid approach is realized to build NEMS and other nanorobotic devices from individual carbon nanotubes and SiGe/Si nanocoils.

18.5.1 Robotic Biomanipulation

Biomanipulation – Autonomous Robotic Pronuclei DNA Injection

To improve the low success rate of manual operation, and to eliminate contamination, an autonomous robotic system (shown in Fig. 18.16) has been developed to deposit DNA into one of the two nuclei of a mouse embryo without inducing cell lysis [18.125, 126]. The laboratory's experimental results show that the success rate for the autonomous embryo pronuclei DNA injection is dramatically improved over manual conventional injection methods. The autonomous robotic system features a hybrid controller that combines visual servoing

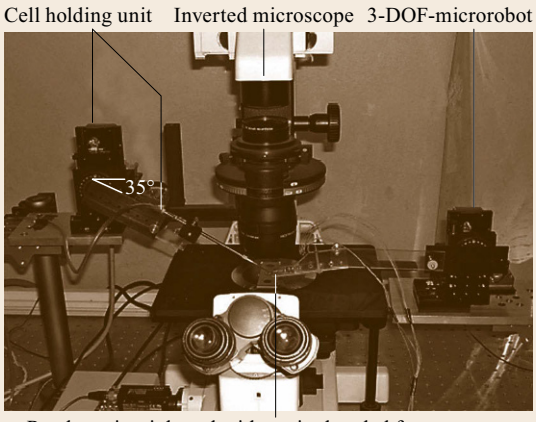

Fig. 18.16 Robotic biomanipulation system with vision and force feedback

and precision position control, pattern recognition for detecting nuclei, and a precise autofocusing scheme. Figure 18.17 illustrates the injection process.

To realize large-scale injection operations, a MEMS cell holder was fabricated using anodic wafer-bonding techniques. Arrays of holes are aligned on the cell holder, which are used to contain and fix individual cells for injection. When well-calibrated, the system with the cell holder makes it possible to inject large numbers of cells using position control. The cell-injection operation can be conducted in a move–inject–move manner.

Successful injection is determined greatly by injection speed and trajectory, and the forces applied to cells (Figure 18.17). To further improve the robotic system's performance, a multi-axial MEMS-based capacitive cellular force sensor is being designed and fabricated to provide real-time force feedback to the robotic system. The MEMS cellular force sensor also aids our research in biomembrane mechanical property characterization.

MEMS-Based Multi-Axis Capacitive Cellular Force Sensor

The MEMS-based two-axis cellular force sensor [18.127] shown in Fig. 18.18 is capable of resolving normal forces applied to a cell as well as tangential forces generated by improperly aligned cell probes. A high-yield microfabrication process was developed to form the 3-D high-aspect-ratio structure using deep reactive ion etching (DRIE) on silicon-on-insulator (SOI) wafers. The constrained outer frame and the inner movable structure are connected by four curved springs. A load applied to the probe causes the inner structure to move, changing the gap between each pair of interdigitated comb capacitors. Consequently, the total capacitance change resolves the applied force. The interdigitated capacitors are orthogonally configured to

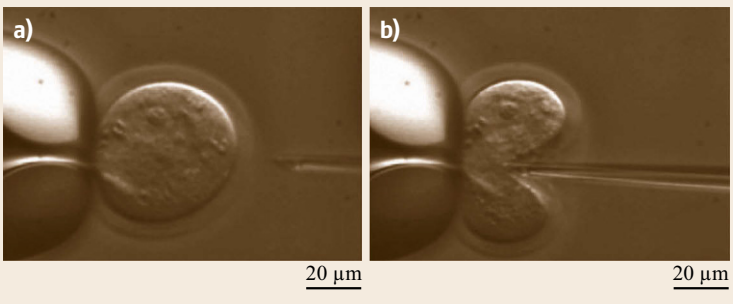

Fig. 18.17a,b Cell injection process. **(a,b)** Cell injection of a mouse oocyte

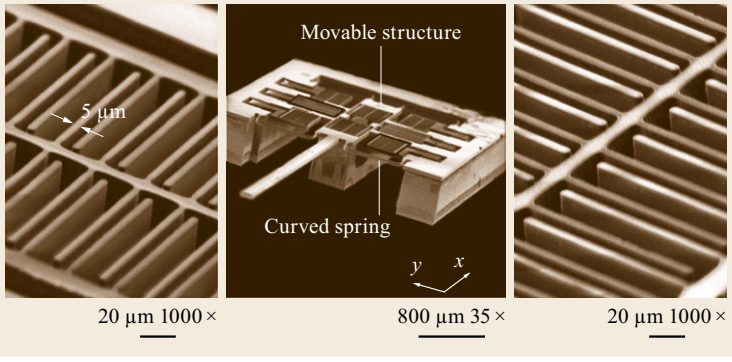

Fig. 18.18 A cellular force sensor with orthogonal comb drives detailed

make the force sensor capable of resolving forces in both the x- and y-directions. The cellular force sensors used in the experiments are capable of resolving forces up to 25 μN with a resolution of 0.01 μN.

Tip geometry affects the quantitative force measurement results. A standard injection pipette (Cook K-MPIP-1000-5) tip section with a tip diameter of 5 μm is attached to the probe of the cellular force sensors.

The robotic system and high-sensitivity cellular force sensor are also applied to biomembrane mechanical property studies [18.128]. The goal is to obtain a general parameterized model describing cell membrane deformation behavior when an external load is applied. This parameterized model serves two chief purposes. First, in robotic biomanipulation, it allows online parameter recognition so that cell membrane deformation behavior can be predicted. Second, for a thermodynamic model of membrane damage in cell injury and recovery studies, it is important to appreciate the mechanical behavior of the membranes. This allows the interpretation of such reported phenomena as mechanical resistance to cellular volume reduction during dehydration, and its relationship to injury. The establishment of such a biomembrane model will greatly facilitate cell injury studies.

Experiments demonstrate that robotics and MEMS technology can play important roles in biological studies such as automating biomanipulation tasks. Aided by robotics, the integration of vision and force-sensing modules, and MEMS design and fabrication techniques, investigations are being conducted in biomembrane mechanical property modeling, deformable cell tracking, and single-cell and biomolecule manipulation.

18.5.2 Nanorobotic Devices

Nanorobotic devices involve tools, sensors, and actuators at the nanometer scale. Shrinking device size makes it possible to manipulate nanosized objects with nanosized tools, measure mass in femtogram ranges, sense force at piconewton scales, and induce GHz motion, among other amazing advancements.

Top-down and bottom-up strategies for manufacturing such nanodevices have been independently investigated by a variety of researchers. Top-down strategies are based on nanofabrication and include technologies such as nanolithography, nanoimprinting, and chemical etching. Presently, these are 2-D fabrication processes with relatively low resolution. Bottom-up strategies are assembly-based techniques. At present, these strategies include such techniques as self-assembly, dip-pen lithography, and directed self-assembly. These techniques can generate regular nanopatterns at large scales. With the ability to position and orient nanometer-scale objects, nanorobotic manipulation is an enabling technology for structuring, characterizing and assembling many types of nanosystems [18.101]. By combining bottom-up and top-down processes, a hybrid nanorobotic approach (as shown in Fig. 18.19) based on nanorobotic manipulation provides a third way to fabricate NEMS by structuring as-grown nanomaterials or nanostructures. This new nanomanufacturing technique can be used to create complex 3-D nanodevices with such building blocks. Nanomaterial science, bionanotechnology, and nanoelectronics will also benefit from advances in nanorobotic assembly.

The configurations of nanotools, sensors, and actuators based on individual nanotubes that have been experimentally demonstrated are summarized as shown in Fig. 18.20.

For detecting deep and narrow features on a surface, cantilevered nanotubes (Fig. 18.20a, [18.103]) have been demonstrated as probe tips for an AFM [18.129], an STM and other types of SPM. Nanotubes provide ultrasmall diameters, ultralarge aspect ratios, and excellent mechanical properties. Manual assembly, direct growth [18.130] and nanoassembly [18.131] have proven effective for their construction. Cantilevered nanotubes have also been demonstrated as probes for the measurement of ultrasmall physical quantities, such as femtogram masses [18.67], mass flow sensors [18.132], and piconewton-order force sensors [18.133] on the basis of their static deflections or change of resonant frequencies detected within an electron microscope. Deflections cannot be measured from micrographs in real time, which limits the application of this kind of sensor. Interelectrode distance changes cause emission current variation of a nanotube emitter and may serve as a candidate to replace microscope images.

Bridged individual nanotubes (Fig. 18.20b, [18.134]) have been the basis for electric characterization. A nanotube-based gas sensor adopted this configuration [18.135].

Opened nanotubes (Fig. 18.20c, [18.136]) can serve as an atomic or molecular container. A thermometer based on this structure has been shown by monitoring the height of the gallium inside the nanotube using TEM [18.137].

Bulk nanotubes can be used to fabricate actuators based on charge-injection-induced bond-length change [18.138], and, theoretically, individual nanotubes also work on the same principle. Electrostatic deflection of a nanotube has been used to construct a relay [18.139]. A new family of nanotube actuators can be constructed by taking advantage of the ultralow inter-layer friction of a multiwalled nanotube. Linear bearings based on telescoping nanotubes have been demonstrated [18.110]. Recently, a micro actu-

ator with a nanotube as a rotation bearing has been demonstrated [18.140]. A preliminary experiment on a promising nanotube linear motor with field emission current serving as position feedback has been shown with nanorobotic manipulation (Fig. 18.20d, [18.136]).

Cantilevered dual nanotubes have been demonstrated as nanotweezers [18.141] and nanoscissors (Fig. 18.20e, [18.91]) by manual and nanorobotic assembly, respectively.

Based on electric resistance change under different temperatures, nanotube thermal probes (Fig. 18.20f) have been demonstrated for measuring the temperature at precise locations. These thermal probes are more advantageous than nanotube-based thermometers because the thermometers require TEM imaging. The probes also have better reproducibility than devices based on dielectrophoretically assembled bulk nanotubes [18.142]. Gas sensors and hot-wire-based mass-flow sensors can also be constructed in this configuration rather than a bridged one.

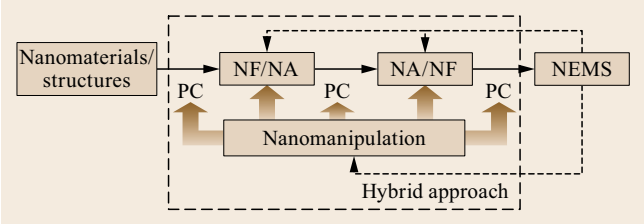

Fig. 18.19 Hybrid approach to NEMS (PC: property characterization, NF: nanofabrication, NA: nanoassembly)

The integration of these devices can be realized using the configurations shown in Figs. 18.20g [18.143] and 18.20h [18.90]. Arrays of individual nanotubes can also be used to fabricate nanosensors, such as position encoders [18.144].

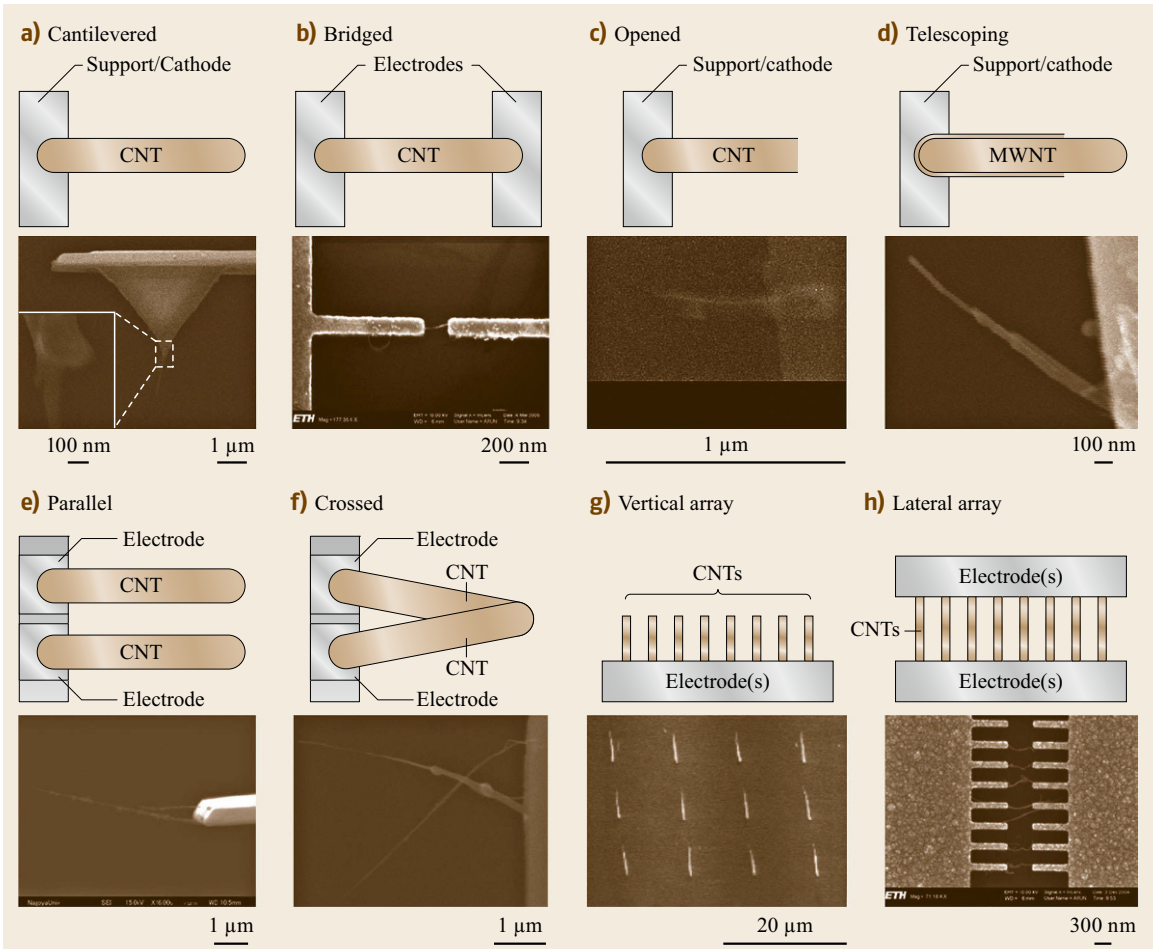

Fig. 18.20a–h Configurations of individual nanotube-based NEMS. *Scale bars*: **(a)** 1 µm (*inset*: 100 nm), **(b)** 200 nm, **(c)** 1 µm, **(d)** 100 nm, **(e)** and **(f)** 1 µm, **(g)** 20 µm, and **(h)** 300 nm. All examples are from the authors' work

Nanotube-based NEMS remains a rich research field with a large number of open problems. New materials and effects at the nanoscale will enable a new family of sensors and actuators for the detection and actuation of ultrasmall quantities or objects with ultrahigh precision and frequencies. Through random spreading, direct growth, and nanorobotic manipulation, prototypes have been demonstrated. However, for integration into NEMS, self-assembly processes will become increasingly important. Among them, we believe that dielectrophoretic nanoassembly will play a significant role for large-scale production of 2-D regular structures.

References

18.1 R.P. Feynman: There's plenty of room at the bottom, Caltech Eng. Sci. **23**, 22–36 (1960)

18.2 M.C. Roco, R.S. Williams, P. Alivisatos: Nanotechnology research directions. In: *Interag. Work. Group Nanosci. Eng. Technol. (IWGN) Workshop Rep.* (Kluwer, Dordrecht 2000)

18.3 Committee on Technology, M.L. Downey, D.T. Moore, G.R. Bachula, D.M. Etter, E.F. Carey, L.A. Perine: *National Nanotechnology Initiative: Leading to the Next Industrial Revolution, A Report by the Interagency Working Group on Nanoscience, Engineering and Technology* (National Science and Technology Council, Washington 2000)

18.4 K. Drexler: *Nanosystems: Molecular Machinery, Manufacturing and Computation* (Wiley Interscience, New York 1992)

18.5 G. Binnig, H. Rohrer, C. Gerber, E. Weibel: Surface studies by scanning tunneling microscopy, Phys. Rev. Lett. **49**, 57–61 (1982)

18.6 W.F. Degrado: Design of peptides and proteins, Adv. Protein Chem. **39**, 51–124 (1998)

18.7 J.-M. Lehn: *Supramolecular Chemistry: Concepts and Perspectives* (VCH, Weinheim 1995)

18.8 G.M. Whitesides, B. Grzybowski: Self-assembly at all scales, Science **295**, 2418–2421 (2002)

18.9 M. Fujita, N. Fujita, K. Ogura, K. Yamaguchi: Spontaneous assembling of ten small components into a three-dimensionally interlocked compound consisting of the same two cage frameworks, Nature **400**, 52–55 (1999)

18.10 T. Ebefors, G. Stemme: Microrobotics. In: *The MEMS Handbook*, ed. by M. Gad-el-Hak (CRC, Boca Raton 2002)

18.11 C.-J. Kim, A.P. Pisano, R.S. Muller: Silicon-processed overhanging microgripper, IEEE/ASME J. MEMS **1**, 31–36 (1992)

18.12 C. Liu, T. Tsao, Y.-C. Tai, C.-M. Ho: Surface micromachined magnetic actuators. In: *Proc. 7th IEEE Int. Conf. Micro Electro Mech. Syst., Oiso* (IEEE, Piscataway 1994) pp. 57–62

18.13 J. Judy, D.L. Polla, W.P. Robbins: A linear piezoelectric stepper motor with submicron displacement and centimeter travel, IEEE Trans. Ultrason. Ferroelectr. Freq. Control **37**, 428–437 (1990)

18.14 K. Nakamura, H. Ogura, S. Maeda, U. Sangawa, S. Aoki, T. Sato: Evaluation of the micro wobbler motor fabricated by concentric buildup process. In: *Proc. 8th IEEE Int. Conf. Micro Electro Mech. Syst., Amsterdam* (IEEE, Piscataway 1995) pp. 374–379

18.15 A. Teshigahara, M. Watanabe, N. Kawahara, I. Ohtsuka, T. Hattori: Performance of a 7-mm microfabricated car, IEEE/ASME J. MEMS **4**, 76–80 (1995)

18.16 K.R. Udayakumar, S.F. Bart, A.M. Flynn, J. Chen, L.S. Tavrow, L.E. Cross, R.A. Brooks, D.J. Ehrlich: Ferroelectric thin-film ultrasonic micromotors. In: *Proc. 4th IEEE Int. Conf. Micro Electro Mech. Syst., Nara* (IEEE, Piscataway 1991) pp. 109–113

18.17 W. Trimmer, R. Jebens: Actuators for micro robots. In: *Proc. 1989 IEEE Int. Conf. Robot. Autom., Scottsdale* (IEEE, Piscataway 1989) pp. 1547–1552

18.18 P. Dario, R. Valleggi, M.C. Carrozza, M.C. Montesi, M. Cocco: Review – Microactuators for microrobots: A critical survey, J. Micromech. Microeng. **2**, 141–157 (1992)

18.19 I. Shimoyama: Scaling in microrobots. In: *Proc. IEEE/RSJ Intell. Robot. Syst., Pittsburgh* (IEEE, Piscataway 1995) pp. 208–211

18.20 R.S. Fearing: Powering 3-dimensional microrobots: power density limitations. In: *Tutorial on Micro Mechatronics and Micro Robotics, Proc. IEEE Int. Conf. Robot. Autom, Leuven*, ed. by G. Girait, P. Dario (IEEE, Piscataway 1998)

18.21 R.G. Gilbertson, J.D. Busch: A survey of microactuator technologies for future spacecraft missions, J. Br. Interplanet. Soc. **49**, 129–138 (1996)

18.22 M. Mehregany, P. Nagarkar, S.D. Senturia, J.H. Lang: Operation of microfabricated harmonic and ordinary side-drive motors. In: *Proc. 3th IEEE Int. Conf. Micro Electro Mech. Syst., Napa Valley* (IEEE, Piscataway 1990) pp. 1–8

18.23 Y.C. Tai, L.S. Fan, R.S. Muller: IC-processed micromotors: design, technology, and testing. In: *Proc. 2nd IEEE Int. Conf. Micro Electro Mech. Syst., Salt Lake City* (IEEE, Piscataway 1989) pp. 1–6

18.24 T. Ohnstein, T. Fukiura, J. Ridley, U. Bonne: Micromachined silicon microvalve. In: *Proc. 3rd IEEE Int. Conf. Micro Electro Mech. Syst., Napa Valley* (IEEE, Piscataway 1990) pp. 95–99

18.25 L.Y. Chen, S.L. Zhang, J.J. Yao, D.C. Thomas, N.C. MacDonald: Selective chemical vapor deposition of tungsten for microdynamic structures. In: *Proc. 2nd IEEE Int. Conf. Micro Electro Mech. Syst., Salt Lake City* (IEEE, Piscataway 1989) pp. 82–87

18.26 K. Yanagisawa, H. Kuwano, A. Tago: An electromagnetically driven microvalve. In: *Proc. 7th Int. Conf. Solid-State Sens. Actuators, Yokohama* (IEEE, Piscataway 1993) pp. 102–105

18.27 S. Brand: New applications of piezo-electric actuators. In: *Proc. 3rd Int. Conf. New Actuators* (Messe

Bremen GmbH, Bremen 1992) p. 59
18.28 M. Esashi, S. Shoji, A. Nakano: Normally close microvalve and micropump fabricated on a silicon wafer. In: *Proc. 4th IEEE Int. Conf. Micro Electro Mech. Syst., Salt Lake City* (IEEE, Piscataway 1989) pp. 29–34
18.29 R. Petrucci, K. Simmons: An introduction to piezoelectric crystals, Sens. Mag. **May**, 26–31 (1994)
18.30 G. Binnig, C.F. Quate, C. Gerber: Atomic force microscope, Phys. Rev. Lett. **56**, 93–96 (1986)
18.31 A. Ashkin, J.M. Dziedzic: Optical trapping and manipulation of viruses and bacteria, Science **235**, 1517–1520 (1987)
18.32 F.H.C. Crick, A.F.W. Hughes: The physical properties of cytoplasm: A study by means of the magnetic particle method, Part I: Experimental, Exp. Cell Res. **1**, 37–80 (1950)
18.33 M.F. Yu, M.J. Dyer, G.D. Skidmore, H.W. Rohrs, X.K. Lu, K.D. Ausman, J.R. Von Ehr, R.S. Ruoff: Three-dimensional manipulation of carbon nanotubes under a scanning electron microscope, Nanotechnology **10**, 244–252 (1999)
18.34 L.X. Dong, F. Arai, T. Fukuda: 3-D nanorobotic manipulation of nano-order objects inside SEM. In: *Proc. 2000 Int. Symp. Micromechatron. Hum. Sci., Nagoya* (IEEE, Piscataway 2000) pp. 151–156
18.35 D.M. Eigler, E.K. Schweizer: Positioning single atoms with a scanning tunneling microscope, Nature **344**, 524–526 (1990)
18.36 P. Avouris: Manipulation of matter at the atomic and molecular levels, Acc. Chem. Res. **28**, 95–102 (1995)
18.37 M.F. Crommie, C.P. Lutz, D.M. Eigler: Confinement of electrons to quantum corrals on a metal surface, Science **262**, 218–220 (1993)
18.38 L.J. Whitman, J.A. Stroscio, R.A. Dragoset, R.J. Cellota: Manipulation of adsorbed atoms and creation of new structures on room-temperature surfaces with a scanning tunneling microscope, Science **251**, 1206–1210 (1991)
18.39 I.-W. Lyo, P. Avouris: Field-induced nanometer-scale to atomic-scale manipulation of silicon surfaces with the STM, Science **253**, 173–176 (1991)
18.40 G. Dujardin, R.E. Walkup, P. Avouris: Dissociation of individual molecules with electrons from the tip of a scanning tunneling microscope, Science **255**, 1232–1235 (1992)
18.41 T.-C. Shen, C. Wang, G.C. Abeln, J.R. Tucker, J.W. Lyding, P. Avouris, R.E. Walkup: Atomic-scale desorption through electronic and vibrational-excitation mechanisms, Science **268**, 1590–1592 (1995)
18.42 M.T. Cuberes, R.R. Schittler, J.K. Gimzewski: Room-temperature repositioning of individual C_60 molecules at Cu steps: Operation of a molecular counting device, Appl. Phys. Lett. **69**, 3016–3018 (1996)
18.43 H.J. Lee, W. Ho: Single-bond formation and characterization with a scanning tunneling microscope, Science **286**, 1719–1722 (1999)
18.44 T. Yamamoto, O. Kurosawa, H. Kabata, N. Shimamoto, M. Washizu: Molecular surgery of DNA based on electrostatic micromanipulation, IEEE Trans. IA **36**, 1010–1017 (2000)
18.45 C. Haber, D. Wirtz: Magnetic tweezers for DNA micromanipulation, Rev. Sci. Instrum. **71**, 4561–4570 (2000)
18.46 D.M. Schäfer, R. Reifenberger, A. Patil, R.P. Andres: Fabrication of two-dimensional arrays of nanometer-size clusters with the atomic force microscope, Appl. Phys. Lett. **66**, 1012–1014 (1995)
18.47 T. Junno, K. Deppert, L. Montelius, L. Samuelson: Controlled manipulation of nanoparticles with an atomic force microscope, Appl. Phys. Lett. **66**, 3627–3629 (1995)
18.48 P.E. Sheehan, C.M. Lieber: Nanomachining, manipulation and fabrication by force microscopy, Nanotechnology **7**, 236–240 (1996)
18.49 C. Baur, B.C. Gazen, B. Koel, T.R. Ramachandran, A.A.G. Requicha, L. Zini: Robotic nanomanipulation with a scanning probe microscope in a networked computing environment, J. Vac. Sci. Technol. B **15**, 1577–1580 (1997)
18.50 R. Resch, C. Baur, A. Bugacov, B.E. Koel, A. Madhukar, A.A.G. Requicha, P. Will: Building and manipulating 3-D and linked 2-D structures of nanoparticles using scanning force microscopy, Langmuir **14**, 6613–6616 (1998)
18.51 J. Hu, Z.-H. Zhang, Z.-Q. Ouyang, S.-F. Chen, M.-Q. Li, F.-J. Yang: Stretch and align virus in nanometer scale on an atomically flat surface, J. Vac. Sci. Technol. B **16**, 2841–2843 (1998)
18.52 M. Sitti, S. Horiguchi, H. Hashimoto: Controlled pushing of nanoparticles: Modeling and experiments, IEEE/ASME Trans. Mechatron. **5**, 199–211 (2000)
18.53 M. Guthold, M.R. Falvo, W.G. Matthews, S. Paulson, S. Washburn, D.A. Erie, R. Superfine, F.P. Brooks Jr., R.M. Taylor II: Controlled manipulation of molecular samples with the nanoManipulator, IEEE/ASME Trans. Mechatron. **5**, 189–198 (2000)
18.54 F. Arai, D. Andou, T. Fukuda: Micro manipulation based on micro physics – strategy based on attractive force reduction and stress measurement. In: *Proc. IEEE/RSJ Int. Conf. Intell. Robot. Syst., Pittsburgh* (IEEE, Piscataway 1995) pp. 236–241
18.55 L.X. Dong, F. Arai, T. Fukuda: 3-D nanorobotic manipulations of nanometer scale objects, J. Robot. Mechatron. **13**, 146–153 (2001)
18.56 H.W.P. Koops, J. Kretz, M. Rudolph, M. Weber, G. Dahm, K.L. Lee: Characterization and application of materials grown by electron-beam-induced deposition, Jpn. J. Appl. Phys. **33**, 7099–7107 (1994)
18.57 S. Iijima: Helical microtubules of graphitic carbon, Nature **354**, 56–58 (1991)
18.58 S.J. Tans, A.R.M. Verchueren, C. Dekker: Room-temperature transistor based on a single carbon nanotube, Nature **393**, 49–52 (1998)
18.59 Y. Huang, X.F. Duan, Y. Cui, L.J. Lauhon, K.-H. Kim, C.M. Lieber: Logic gates and computation from as-

sembled nanowire building blocks, Science **294**, 1313–1317 (2001)
18.60 A. Bachtold, P. Hadley, T. Nakanishi, C. Dekker: Logic circuits with carbon nanotube transistors, Science **294**, 1317–1320 (2001)
18.61 R.H. Baughman, A.A. Zakhidov, W.A. de Heer: Carbon nanotubes – the route toward applications, Science **297**, 787–792 (2002)
18.62 N. Wang, Z.K. Tang, G.D. Li, J.S. Chen: Single-walled 4 Å carbon nanotube arrays, Nature **408**, 50–51 (2000)
18.63 Z.W. Pan, S.S. Xie, B.H. Chang, C.Y. Wang, L. Lu, W. Liu, W.Y. Zhou, W.Z. Li, L.X. Qian: Very long carbon nanotubes, Nature **394**, 631–632 (1998)
18.64 H.W. Zhu, C.L. Xu, D.H. Wu, B.Q. Wei, R. Vajtai, P.M. Ajayan: Direct synthesis of long single-walled carbon nanotube strands, Science **296**, 884–886 (2002)
18.65 M.J. Treacy, T.W. Ebbesen, J.M. Gibson: Exceptionally high Young's modulus observed for individual carbon nanotubes, Nature **381**, 678–680 (1996)
18.66 E.W. Wong, P.E. Sheehan, C.M. Lieber: Nanobeam mechanics: Elasticity, strength, and toughness of nanorods and nanotubes, Science **277**, 1971–1975 (1997)
18.67 P. Poncharal, Z.L. Wang, D. Ugarte, W.A. de Heer: Electrostatic deflections and electromechanical resonances of carbon nanotubes, Science **283**, 1513–1516 (1999)
18.68 M.F. Yu, O. Lourie, M.J. Dyer, K. Moloni, T.F. Kelley, R.S. Ruoff: Strength and breaking mechanism of multiwalled carbon nanotubes under tensile load, Science **287**, 637–640 (2000)
18.69 A. Krishnan, E. Dujardin, T.W. Ebbesen, P.N. Yianilos, M.M.J. Treacy: Young's modulus of single-walled nanotubes, Phys. Rev. B **58**, 14–013–14–019 (1998)
18.70 J.P. Salvetat, G.A.D. Briggs, J.-M. Bonard, R.R. Bacsa, A.J. Kulik, T. Stockli, N.A. Burnham, L. Forro: Elastic and shear moduli of single-walled carbon nanotube ropes, Phys. Rev. Lett. **82**, 944–947 (1999)
18.71 M.F. Yu, B.S. Files, S. Arepalli, R.S. Ruoff: Tensile loading of ropes of single wall carbon nanotubes and their mechanical properties, Phys. Rev. Lett. **84**, 5552–5555 (2000)
18.72 D.A. Walters, L.M. Ericson, M.J. Casavant, J. Liu, D.T. Colbert, K.A. Smith, R.E. Smalley: Elastic strain of freely suspended single-wall carbon nanotube ropes, Appl. Phys. Lett. **74**, 3803–3805 (1999)
18.73 R. Saito, M. Fujita, G. Dresselhaus, M.S. Dresselhaus: Electronic structure of graphene tubules based on C_{60}, Phys. Rev. B **46**, 1804–1811 (1992)
18.74 T.W. Ebbesen, H.J. Lezec, H. Hiura, J.W. Bennett, H.F. Ghaemi, T. Thio: Electrical conductivity of individual carbon nanotubes, Nature **382**, 54–56 (1996)
18.75 H.J. Dai, E.W. Wong, C.M. Lieber: Probing electrical transport in nanomaterials: conductivity of individual carbon nanotubes, Science **272**, 523–526 (1996)
18.76 P. Kim, L. Shi, A. Majumdar, P.L. McEuen: Thermal transport measurements of individual multiwalled nanotubes, Phys. Rev. Lett. **87**, 215502 (2001)
18.77 W.J. Liang, M. Bockrath, D. Bozovic, J.H. Hafner, M. Tinkham, H. Park: Fabry–Perot interference in a nanotube electron waveguide, Nature **411**, 665–669 (2001)
18.78 S. Frank, P. Poncharal, Z.L. Wang, W.A. de Heer: Carbon nanotube quantum resistors, Science **280**, 1744–1746 (1998)
18.79 X.B. Zhang, D. Bernaerts, G. Van Tendeloo, S. Amelincks, J. Van Landuyt, V. Ivanov, J.B. Nagy, P. Lambin, A.A. Lucas: The texture of catalytically grown coil-shaped carbon nanotubules, Europhys. Lett. **27**, 141–146 (1994)
18.80 X.Y. Kong, Z.L. Wang: Spontaneous polarization-induced nanohelixes, nanosprings, and nanorings of piezoelectric nanobelts, Nano Lett. **3**, 1625–1631 (2003)
18.81 S.V. Golod, V.Y. Prinz, V.I. Mashanov, A.K. Gutakovsky: Fabrication of conducting GeSi/Si micro- and nanotubes and helical microcoils, Semicond. Sci. Technol. **16**, 181–185 (2001)
18.82 L. Zhang, E. Deckhardt, A. Weber, C. Schönenberger, D. Grützmacher: Controllable fabrication of SiGe/Si and SiGe/Si/Cr helical nanobelts, Nanotechnology **16**, 655–663 (2005)
18.83 D.J. Bell, L.X. Dong, Y. Sun, L. Zhang, B.J. Nelson, D. Grützmacher: Manipulation of nanocoils for nanoelectromagnets. In: *Proc. 5th IEEE Conf. Nanotechnol., Nagoya* (IEEE, Piscataway 2005) pp. 149–152
18.84 D.J. Bell, Y. Sun, L. Zhang, L.X. Dong, B.J. Nelson, D. Grützmacher: Three-dimensional nanosprings for electromechanical sensors. In: *Proc. 13th Int. Conf. Solid-State Sens. Actuators Microsyst., Seoul* (IEEE, Piscataway 2005) pp. 15–18
18.85 S. Iijima, T. Ichihashi: Single-shell carbon nanotubes of 1-nm diameter, Nature **363**, 603–605 (1993)
18.86 D.S. Bethune, C.H. Kiang, M.S. de Vries, G. Gorman, R. Savoy, J. Vazquez, R. Beyers: Cobalt-catalysed growth of carbon nanotubes with single-atomic-layer walls, Nature **363**, 605–607 (1993)
18.87 R. Martel, T. Schmidt, H.R. Shea, T. Hertel, P. Avouris: Single- and multi-wall carbon nanotube field-effect transistors, Appl. Phys. Lett. **73**, 2447–2449 (1998)
18.88 N.R. Franklin, Y.M. Li, R.J. Chen, A. Javey, H.J. Dai: Patterned growth of single-walled carbon nanotubes on full 4-inch wafers, Appl. Phys. Lett. **79**, 4571–4573 (2001)
18.89 T. Rueckes, K. Kim, E. Joselevich, G.Y. Tseng, C.-L. Cheung, C.M. Lieber: Carbon nanotube-based non-volatile random access memory for molecular computing, Science **289**, 94–97 (2000)
18.90 A. Subramanian, B. Vikramaditya, L.X. Dong, D. Bell, B.J. Nelson: Micro and nanorobotic assembly using dielectrophoresis. In: *Robotics:*

Science and Systems I, ed. by S. Thrun, G.S. Sukhatme, S. Schaal, O. Brock (MIT Press, Cambridge 2005) pp. 327–334
18.91 T. Fukuda, F. Arai, L.X. Dong: Assembly of nanodevices with carbon nanotubes through nanorobotic manipulations, Proc. IEEE **91**, 1803–1818 (2003)
18.92 M.R. Falvo, G.J. Clary, R.M. Taylor, V. Chi, F.P. Brooks, S. Washburn, R. Superfine: Bending and buckling of carbon nanotubes under large strain, Nature **389**, 582–584 (1997)
18.93 H.W.C. Postma, A. Sellmeijer, C. Dekker: Manipulation and imaging of individual single-walled carbon nanotubes with an atomic force microscope, Adv. Mater. **12**, 1299–1302 (2000)
18.94 H.W.C. Postma, M. de Jonge, Z. Yao, C. Dekker: Electrical transport through carbon nanotube junctions created by mechanical manipulation, Phys. Rev. B **62**, R10653–R10656 (2000)
18.95 T. Hertel, R. Martel, P. Avouris: Manipulation of individual carbon nanotubes and their interaction with surfaces, J. Phys. Chem. B **102**, 910–915 (1998)
18.96 P. Avouris, T. Hertel, R. Martel, T. Schmidt, H.R. Shea, R.E. Walkup: Carbon nanotubes: nanomechanics, manipulation, and electronic devices, Appl. Surf. Sci. **141**, 201–209 (1999)
18.97 L. Roschier, J. Penttila, M. Martin, P. Hakonen, M. Paalanen, U. Tapper, E.I. Kauppinen, C. Journet, P. Bernier: Single-electron transistor made of multiwalled carbon nanotube using scanning probe manipulation, Appl. Phys. Lett. **75**, 728–730 (1999)
18.98 M. Ahlskog, R. Tarkiainen, L. Roschier, P. Hakonen: Single-electron transistor made of two crossing multiwalled carbon nanotubes and its noise properties, Appl. Phys. Lett. **77**, 4037–4039 (2000)
18.99 M.R. Falvo, R.M. Taylor II, A. Helser, V. Chi, F.P. Brooks Jr, S. Washburn, R. Superfine: Nanometre-scale rolling and sliding of carbon nanotubes, Nature **397**, 236–238 (1999)
18.100 M.R. Falvo, J. Steele, R.M. Taylor II, R. Superfine: Gearlike rolling motion mediated by commensurate contact: Carbon nanotubes on HOPG, Phys. Rev. B **62**, R10665–R10667 (2000)
18.101 L.X. Dong: *Nanorobotic Manipulations of Carbon Nanotubes*, Ph.D. Thesis (Nagoya University, Nagoya 2003)
18.102 J.H. Hafner, C.-L. Cheung, T.H. Oosterkamp, C.M. Lieber: High-yield assembly of individual single-walled carbon nanotube tips for scanning probe microscopies, J. Phys. Chem. B **105**, 743–746 (2001)
18.103 L.X. Dong, F. Arai, T. Fukuda: Electron-beam-induced deposition with carbon nanotube emitters, Appl. Phys. Lett. **81**, 1919–1921 (2002)
18.104 L.X. Dong, F. Arai, T. Fukuda: 3-D nanorobotic manipulations of multi-walled carbon nanotubes. In: *Proc. 2001 IEEE Int. Conf. Robot. Autom. (ICRA2001), Seoul* (IEEE, Piscataway 2001) pp. 632–637
18.105 L.X. Dong, F. Arai, T. Fukuda: Three-dimensional nanorobotic manipulations of carbon nanotubes, J. Robot. Mechatron. JSME **14**, 245–252 (2002)
18.106 L.X. Dong, F. Arai, T. Fukuda: Inter-process measurement of MWNT rigidity and fabrication of MWNT junctions through nanorobotic manipulations. In: *Conf. Proc. Nanonetw. Mater. Fuller. Nanotub. Relat. Mater.*, Vol. 590, (AIP, Melville 2001) pp. 71–74
18.107 L.X. Dong, F. Arai, T. Fukuda: Shape modification of carbon nanotubes and its applications in nanotube scissors. In: *Proc. IEEE Int. Conf. Nanotechnol. (IEEE-NANO2002), Washington* (IEEE, Piscataway 2002) pp. 443–446
18.108 L.X. Dong, F. Arai, T. Fukuda: Destructive constructions of nanostructures with carbon nanotubes through nanorobotic manipulations, IEEE/ASME Trans. Mechatron. **9**, 350–357 (2004)
18.109 J. Cumings, P.G. Collins, A. Zettl: Peeling and sharpening multiwall nanotubes, Nature **406**, 58 (2000)
18.110 J. Cumings, A. Zettl: Low-friction nanoscale linear bearing realized from multiwall carbon nanotubes, Science **289**, 602–604 (2000)
18.111 L.X. Dong, F. Arai, T. Fukuda: 3-D nanoassembly of carbon nanotubes through nanorobotic manipulations. In: *Proc. 2002 IEEE Int. Conf. Robot. Autom. (ICRA2002), Washington* (IEEE, Piscataway 2002) pp. 1477–1482
18.112 L.X. Dong, F. Arai, T. Fukuda: Mechanochemical nanorobotic manipulations of carbon nanotubes, Jpn. J. Appl. Phys. **42**, 295–298 (2003)
18.113 R. Saito, G. Dresselhaus, M.S. Dresselhaus: Tunneling conductance of connected carbon nanotubes, Phys. Rev. B **53**, 2044–2050 (1996)
18.114 L. Chico, V.H. Crespi, L.X. Benedict, S.G. Louie, M.L. Cohen: Pure carbon nanoscale devices: nanotube heterojunctions, Phys. Rev. Lett. **76**, 971–974 (1996)
18.115 M. Menon, D. Srivastava: Carbon nanotube *T junctions*: nanoscale metal–semiconductor–metal contact devices, Phys. Rev. Lett. **79**, 4453–4456 (1997)
18.116 Z. Yao, H.W.C. Postma, L. Balents, C. Dekker: Carbon nanotube intramolecular junctions, Nature **402**, 273–276 (1999)
18.117 H.W.C. Postma, T. Teepen, Z. Yao, M. Grifoni, C. Dekker: Carbon nanotube single-electron transistors at room temperature, Science **293**, 76–79 (2001)
18.118 M.S. Fuhrer, L. Shih, M. Forero, Y.-G. Yoon, M.S.C. Mazzoni, H.J. Choi, J. Ihm, S.G. Louie, A. Zettl, P.L. McEuen: Crossed nanotube junctions, Science **288**, 494–497 (2000)
18.119 T. Rueckes, K. Kim, E. Joselevich, G.Y. Treng, C.L. Cheung, C.M. Lieber: Carbon nanotube-based nonvolatile random access memory for molecular computing science, Science **289**, 94–97 (2000)
18.120 A.G. Rinzler, J.H. Hafner, P. Nikolaev, L. Lou, S.G. Kim, D. Tománek, P. Nordlander, D.T. Colbert, R.E. Smalley: Unraveling nanotubes: field emission from an atomic wire, Science **269**, 1550–1553

(1995)
18.121 Y. Saito, K. Hamaguchi, K. Hata, K. Uchida, Y. Tasaka, F. Ikazaki, M. Yumura, A. Kasaya, Y. Nishina: Conical beams from open nanotubes, Nature **389**, 554 (1997)
18.122 S.C. Minne, G. Yaralioglu, S.R. Manalis, J.D. Adams, J. Zesch, A. Atalar, C.F. Quate: Automated parallel high-speed atomic force microscopy, Appl. Phys. Lett. **72**, 2340–2342 (1998)
18.123 G.D. Skidmore, E. Parker, M. Ellis, N. Sarkar, R. Merkle: Exponential assembly, Nanotechnology **11**, 316–321 (2001)
18.124 Y. Cui, Q.Q. Wei, H.K. Park, C.M. Lieber: Nanowire nanosensors for highly sensitive and selective detection of biological and chemical species, Science **293**, 1289–1292 (2001)
18.125 Y. Sun, B.J. Nelson: Microrobotic cell injection. In: *Proc. 2001 IEEE Int. Conf. Robot. Autom. (ICRA2001), Seoul* (IEEE, Piscataway 2001) pp. 620–625
18.126 Y. Sun, B.J. Nelson: Autonomous injection of biological cells using visual servoing. In: *Int. Symp. Exp. Robot. (ISER)* (Lecture Notes Control Inform. Sci., Hawaii 2000) pp. 175–184
18.127 Y. Sun, B.J. Nelson, D.P. Potasek, E. Enikov: A bulk microfabricated multi-axis capacitive cellular force sensor using transverse comb drives, J. Micromech. Microeng. **12**, 832–840 (2002)
18.128 Y. Sun, K. Wan, K.P. Roberts, J.C. Bischof, B.J. Nelson: Mechanical property characterization of mouse zona pellucida, IEEE Trans. Nanobiosci. **2**, 279–286 (2003)
18.129 H.J. Dai, J.H. Hafner, A.G. Rinzler, D.T. Colbert, R.E. Smalley: Nanotubes as nanoprobes in scanning probe microscopy, Nature **384**, 147–150 (1996)
18.130 J.H. Hafner, C.L. Cheung, C.M. Lieber: Growth of nanotubes for probe microscopy tips, Nature **398**, 761–762 (1999)
18.131 H. Nishijima, S. Kamo, S. Akita, Y. Nakayama, K.I. Hohmura, S.H. Yoshimura, K. Takeyasu: Carbon-nanotube tips for scanning probe microscopy: preparation by a controlled process and observation of deoxyribonucleic acid, Appl. Phys. Lett. **74**, 4061–4063 (1999)
18.132 L.X. Dong, F. Arai, M. Nakajima, P. Liu, T. Fukuda: Nanotube devices fabricated in a nano laboratory. In: *Proc. 2003 IEEE Int. Conf. Robot. Autom. (ICRA2003), Taipei* (IEEE, Piscataway 2003) pp. 3624–3629
18.133 M. Nakajima, F. Arai, L.X. Dong, T. Fukuda: Pico-Newton order force measurement using a calibrated carbon nanotube probe inside a scanning electron microscope, J. Robot. Mechatron. JSME **16**(2), 155–162 (2004)
18.134 A. Subramanian, B.J. Nelson, L.X. Dong, D. Bell: Dielectrophoretic nanoassembly of nanotube-based NEMS with nanoelectrodes. In: *6th IEEE Int. Symp. Assem. Task Plan., Montréal* (IEEE, Piscataway 2005) pp. 200–205
18.135 J. Kong, N.R. Franklin, C.W. Zhou, M.G. Chapline, S. Peng, K.J. Cho, H.J. Dai: Nanotube molecular wires as chemical sensors, Science **287**, 622–625 (2000)
18.136 L.X. Dong, B.J. Nelson, T. Fukuda, F. Arai: Towards linear nano servomotors with integrated position sensing. In: *Proc. 2005 IEEE Int. Conf. Robot. Autom., Barcelona* (IEEE, Piscataway 2005) pp. 867–872
18.137 Y.H. Gao, Y. Bando: Carbon nanothermometer containing gallium, Nature **415**, 599 (2002)
18.138 R.H. Baughman, C.X. Cui, A.A. Zakhidov, Z. Iqbal, J.N. Barisci, G.M. Spinks, G.G. Wallace, A. Mazzoldi, D. De Rossi, A.G. Rinzler, O. Jaschinski, S. Roth, M. Kertesz: Carbon nanotube actuators, Science **284**, 1340–1344 (1999)
18.139 S.W. Lee, D.S. Lee, R.E. Morjan, S.H. Jhang, M. Sveningsson, O.A. Nerushev, Y.W. Park, E.E.B. Campbell: A three-terminal carbon nanorelay, Nano Lett. **4**, 2027–2030 (2004)
18.140 A.M. Fennimore, T.D. Yuzvinsky, W.-Q. Han, M.S. Fuhrer, J. Cumings, A. Zettl: Rotational actuators based on carbon nanotubes, Nature **424**, 408–410 (2003)
18.141 P. Kim, C.M. Lieber: Nanotube nanotweezers, Science **286**, 2148–2150 (1999)
18.142 C.K.M. Fung, V.T.S. Wong, R.H.M. Chan, W.J. Li: Dielectrophoretic batch fabrication of bundled carbon nanotube thermal sensors, IEEE Trans. Nanotech. **3**, 395–403 (2004)
18.143 A. Subramanian, L.X. Dong, B.J. Nelson: Selective eradication of individual nanotubes from vertically aligned arrays. In: *Proc. 2005 IEEE/ASME Int. Conf. Adv. Intell. Mechatron., Monterey* (IEEE, Piscataway 2005) pp. 105–110
18.144 L.X. Dong, A. Subramanian, B.J. Nelson: Nano encoders based on arrays of single nanotube emitter. In: *Proc. 5th IEEE Conf. Nanotechnol., Nagoya* (IEEE, Piscataway 2005) pp. 211–214